UNIVERSITEIT • STELLENBOSCH • UNIVERSITY

The Feedback Control Of A Robotic Gymnast

by

Henry Kotzé

Mechatronic Project 448

Report submitted in partial fulfilment of the requirements of the module Mechatronic Project 448 for the degree Baccalaureus in Engineering in the Department of Mechanical and Mechatronic Engineering at the University of Stellenbosch

Study leader: Dr. J.A.A Engelbrecht

October 2018

Plagiarism Declaration

I have read and understand the Stellenbosch University Policy on Plagiarism and the definitions of plagiarism and self-plagiarism contained in the Policy [Plagiarism: The use of the ideas or material of others without acknowledgement, or the re-use of one's own previously evaluated or published material without acknowledgement or indication thereof (self-plagiarism or text-recycling)].

I also understand that direct translations are plagiarism, unless accompanied by an appropriate acknowledgement of the source. I also know that verbatim copy that has not been explicitly indicated as such, is plagiarism.

I know that plagiarism is a punishable offence and may be referred to the University's Central Disciplinary Committee (CDC) who has the authority to expel me for such an offence.

I know that plagiarism is harmful for the academic environment and that it has a negative impact on any profession.

Accordingly all quotations and contributions from any source whatsoever (including the internet) have been cited fully (acknowledged); further, all verbatim copies have been expressly indicated as such (e.g. through quotation marks) and the sources are cited fully.

I declare that, except where a source has been cited, the work contained in this assignment is my own work and that I have not previously (in its entirety or in part) submitted it for grading in this module/assignment or another module/assignment.

I declare that have not allowed, and will not allow, anyone to use my work (in paper, graphics, electronic, verbal or any other format) with the intention of passing it off as his/her own work.

I know that a mark of zero may be awarded to assignments with plagiarism and also that no opportunity be given to submit an improved assignment.

Name: ____________________
Student No: ____________________
Signature: ____________________
Date: ____________________

Abstract

The Feedback Control of a Robotic Gymnast

H. Kotzé

Department of Mechanical and Mechatronic Engineering,
University of Stellenbosch,
Private Bag X1, Matieland 7602, South Africa.

Thesis: BEng (Mechatronics)

October 2018

This report presents the design, implementation, and testing of a feedback control system for a robotic gymnast. Feedback control systems were designed to swing up and balance an under-actuated robotic gymnast system. A physical system, consisting of mechanical and electronic hardware, was designed and constructed, and the feedback controllers were implemented in software. The feedback control system was verified both in simulation and on the physical system..

Uittreksel

Die Terugvoer Beheerwet van 'n Robotiese Gimnas

("The Feedback Control of a Robotic Gymnast")

H. Kotzé

Departement Meganiese en Megatroniese Ingenieurswese,
Universiteit van Stellenbosch,
Privaatsak X1, Matieland 7602, Suid Afrika.

Tesis: BIng (Megatronika)

Oktober 2018

In die projek word die swaaiende en balanseering beheerwette vir 'n robotiese gimnas genavors, ontwerp en getoets op 'n fisiese model. Die eletroniese, meganiese en sagteware ontwerpe word bespreek om ten einde te wys hoe die fisiese model, beheerders en so voort geimplementeer en getoets is.

Executive Summary

Executive Summary
Project Title
mewe
Objectives
adsad
Which aspects of the project are unique?
asdasd
What are the (expected) findings?
ddd
What value do the results have?
ddd
If more than one student is involved, what is each one's contribution?
ddd
Which aspects of the project will carry on after completion?
ddd
What are the expected advantages of continuation?
ddd
What arrangements have been made to expedite continuation?
ddd

ECSA Outcome Evaluation

Problem Solving:
Application of Scientific and Engineering Knowledge:
Engineering Design:
Engineering Methods, Skills and Tools:
Professional and Technical Communication: Individual, Team and Multidisciplinary Working: Independent Learning Ability:

Acknowledgements

I would like to express my sincere gratitude to the following people and organisations.

Dr. Japie Engelbrecht for supervising the project throughout the year. He provided critical feedback on progress, guided me in the correct direction and was a voice of reason throughout the project.

The Electrical and Electronic Department for allowing the use of their equipment and facilities. They allowed me to work with confidence ensuring the facilities and equipment are maintained with no interruption to my work.

Mr. Croukamp, Mr. van Eenden and Mr. Lecholo for assisting me with the mechanical and electronic designs. The atmosphere in the manufacturing labotorium was always welcoming.

The group of final year student working together in the 4th floor labs. You all made the experience more worthwhile and encouraged me through difficult times.

Contents

List of Figures

List of Tables

Nomenclature

Constants

g =	$9.81\,\mathrm{m/s^2}$	

Variables

I	Inertia	[$\mathrm{kg{\cdot}m^2}$]
m	mass	[kg]
l	Lenght	[m]
L	Lenght	[m]
R	Reaction Force	[N]
x	Coordinate	[m]
$\ddot{x}$	Acceleration	[$\mathrm{m/s^2}$]
θ	Rotation angle	[rad]
ϕ	Rotation angle	[rad]
τ	Torque	[$\mathrm{N{\cdot}m}$]

Vectors and Tensors

$\overrightarrow{\boldsymbol{q}}$	Physical vector, see equation ()...

Subscripts

a	Unactuated Pendulum
b	Actuated Pendulum
1	Unactuated Pendulum center of mass
2	Actuated Pendulum center of mass

Chapter 1

Introduction

1.1 Problem Statement

In this report a feedback control system for a robotic gymnast that is able to swing from the "hanging" position to the "handstand" position will be designed, implemented and verified. Feedback control loops must be designed that use the "legs" of the gymnast to swing the "body" of the gymnast from the "hanging" position to a "handstand" position and then balance the gymnast on top of the horizontal bar. A mathematical model for the dynamics of the swinging robotic gymnast system must be derived or sourced from literature. The dynamics are analysed to propose an appropriate feedback control architecture that actuates the "legs" of the gymnast using feedback from sensors that measure the swinging motion of the gymnast on a horizontal bar. A practical demonstrator must be constructed and the correct operation must be demonstrated.

1.2 The Robotic Gymnast System

Figure 1.1 provides an overview of the system to create a mental picture for the variables and concepts used throughout the report. There are 2 pendulums that are attach together with a hinge. At this hinge there is a torque being applied by a motor to the actuated pendulum. The entire system rotates around the fixed hinge at the top to which the unactuated pendulum is connected. The system is describe using two independent parameters, θ and ϕ which describes the entire system.

The goal is to use the feedback of the independent parameters to apply a torque to the actuated pendulum to swing the gymnast from the hanging position and balance in the inverted position. This is accomplished by designing a microcontroller to interface with sensors to provide information about the

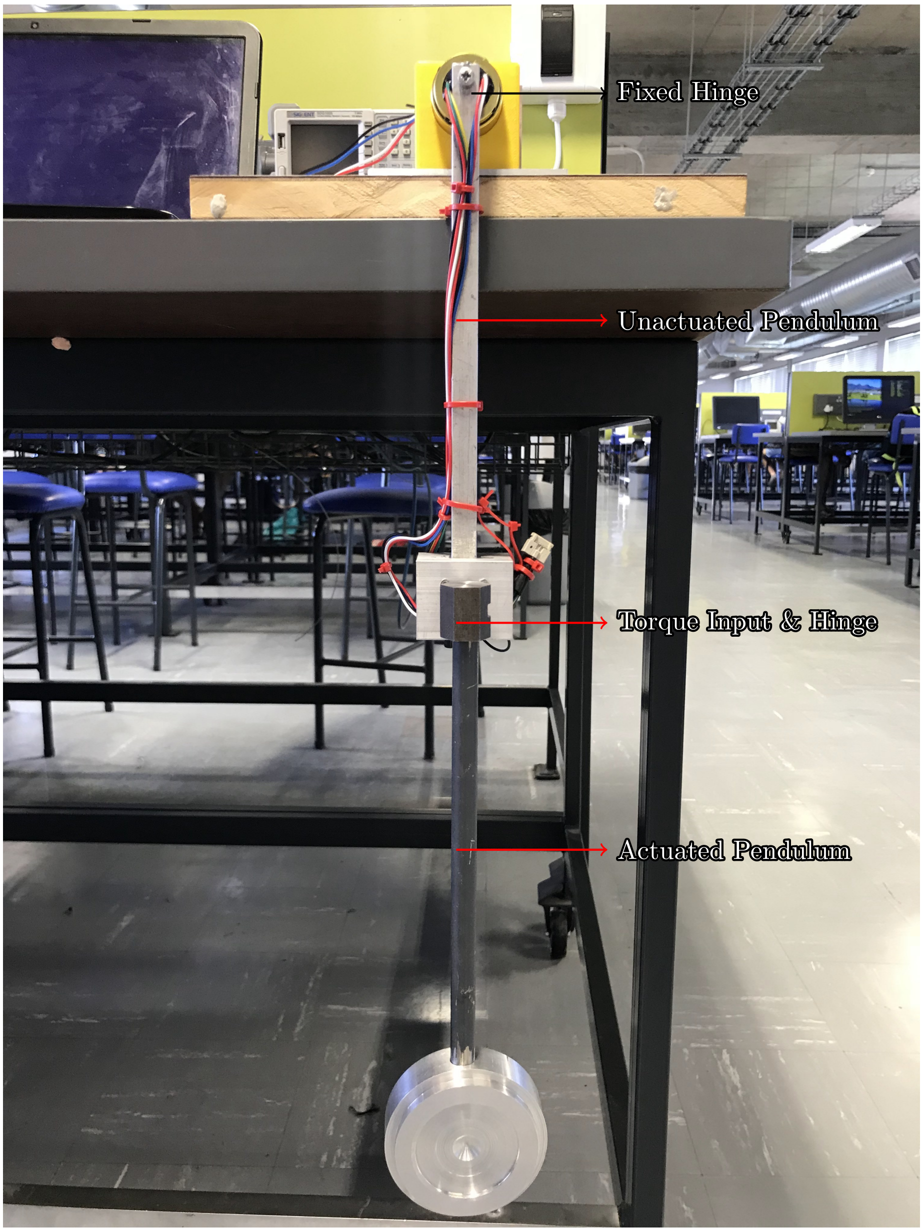

Figure 1.1: Overview of the Robotic Gymnast System

independent parameters and implement the control laws for the balancing and swinging in software.

1.3 Literature Study

A literature study was performed to survey different physical implementations of the system, different approaches to modelling the dynamics, different physical implementations of the system, and different techniques to perform the feedback control to perform the swing-up and the balancing of the robotic gymnast.

Previous attempts to swing up and balance the robotic gymnast used two separate controllers. The first controller is responsible for swinging the robotic gymnast from the hanging position up towards the inverted position. When the swing-up controller brought the gymnast near the inverted position, a new controller is used balance the gymnast. The different types of swing up and balancing controllers used by previous researchers are summarised below, followed by a decision on the approaches selected for this project..

Spong (1995) implemented the swing-up controller by using partial feedback linearisation which results in a linear response from either the *actuated* or *unactuated* pendulum. Using *non-collocated* linearisation he was able to control the *unactuated* pendulum to follow a desired trajectory and used the phase portrait of the zero dynamics of the system to show that the closed-loop system will converge to the inverted equilibrium position. Spong also demonstrated how the swing-up can be achieved by using *collocated* linearisation which linearises the response of the *actuated* pendulum. This allows the actuated pendulum to follow a desired trajectory and Spong provides a energy-based trajectory that increases the energy in the system. Once the both swing up controller brings the system to the inverted balancing position, the feedback control system switches over to a linear quadratic regulator (LQR) to balance the system.

Brown and Passino (1997) provided two manually tuned nonlinear controllers for the balancing of the robotic gymnast and tested and compared them against a designed LQR controller. The two nonlinear controller were a direct fuzzy controller (DFC) and a fuzzy model reference learning controller (FMRLC). The gains for the DFC controller were based on the gains of the LQR controller. The DFC controller was implemented and successfully balanced the gymnast. However the LQR controller provided smoother state trajectories and smaller control input. The FMRLC uses no explicit dynamical reference model and instead the outputs of the plant using normalising gains are directly fed into the second fuzzy system. The FMRLC controller was a significant improvement on the DFC, but yet again did not perform as well as the LQR controller.

Brown and Passino also attempted to swing the acrobat to the inverted balancing position using the energy based trajectory proposed by Spong, but without the partial linearisation feedback. Brown and Passino were able to swing and balance the acrobat using this approach,but their approach resulted in larger input signals that were not as smooth as the input signals when using partial feedback linearisation.

In most of the literature, the mathematical model of the robotic gymnast is derived using the Euler-Lagrangian equation. This approach is used because the mechanical energy in the system is easily identified. Lehl (2012) and Tedrake (2009) both derived the simplified mathematical models for the robotic gymnast using point mass approximations.

Based on the literature study, it was decided to perform the swing up control using partial feedback linearisation and an energy-based reference trajectory, and to perform the balancing control using a linear full state feedback controller.

1.4 System Overview

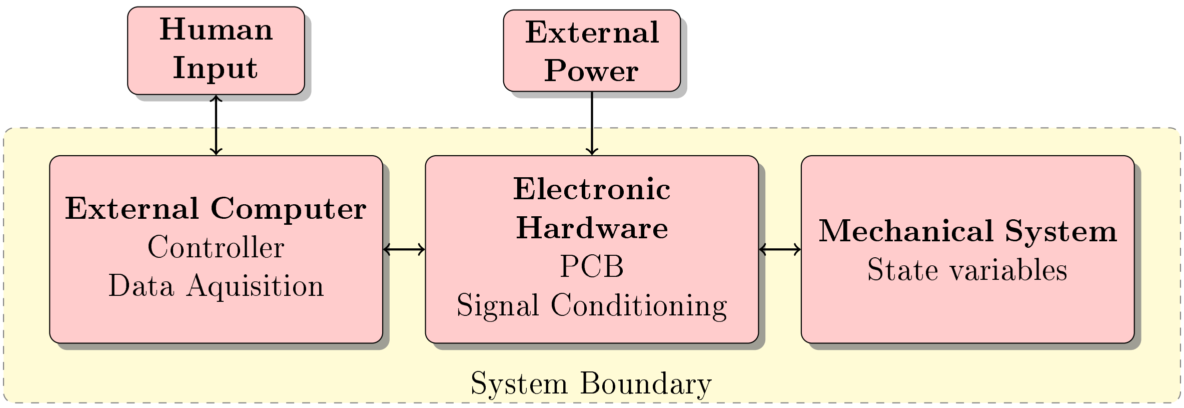

Figure 1.2: System Overview of the Feedback Control of Robotic Gymnast

Figure 1.2 provides an overview of the system that was developed in this project , and shows the individual subsystems with their internal and external interfaces. The individual subsystems could be developed separately with well-defined interfaces to one another. A brief overview of each subsystem is presented here.

The external computer executes the feedback control laws that perform the swing up and balancing, and supplies the commands for the motor actuator based on sensor feedback from the angle sensors for both the actuated and the non-actuated pendulums. This allows for the verification of system parameters, debugging and experimental tests.

The electronic hardware acts as the interface between external computer and the robotic gymnast mechanical hardware. The external computer communicates with the electronic hardware using serial communications to send commands and to receive data. The electronic hardware interfaces directly with the motor actuator using a motor driver, and interfaces with the angle sensors using digital and analog interfaces. The electronic hardware is implemented on a printed circuit board (PCB).

A mechanical prototype system was designed and constructed. The mechanical system consists of the mechanical structure of the robotic gymnast, the motor actuator, and the angle sensors for the two pendulum links (unactuated and actuated). The motor actuator is controlled by the electronic hardware based on commands provided by the external computer, and the two angle sensors are read by the electronic hardware, and their measurements are transmitted back to the external computer.

The external interfaces to the system include the power supplied to the system and the input commands provided by the user.

1.5 Project Execution

The project was executed in a sequence of steps in order to achieve the results as presented in the report. It is presented to provide the reader with an understanding of how the individual subsystems were developed individually and eventual ly integrated into the full system.

First the mathematical model of the system was derived by using the appropriate approach. The derived mathematical model was then implemented on a simulation program where the dynamics of the system was verified and inspected.

Following the successful implementation of the mathematical model the various controllers were designed and implemented on the simulation program. The behaviour of the simulated responses were inspected and analysed.

The simulation provided the specification for the mechanical design to commence and created the physical model that provided an acceptable representation of the mathematical model.

During manufacturing of the mechanical design the electronic design started. Conceptual designs were created capable of meeting the requirements and the selected design was manufactured. The electronic design was then tested to ensure it performs as designed with the opportunity to create revisions.

Following the successful testing of the electronic design, the programming of the microcontroller and external computer started. This included the programming of the controller, data acquisition system and the conversions of the sampled data.

Once the microcontroller could provide the external computer with system state information, the system identification tests occurred to determine the various system parameters. These new system parameters were used in the simulation program to update the existing controllers and verify the responses in simulation.

The updated controllers were then implemented onto the external computer for the system experiments to start. From these system experiments the response of the experiments were compared to those of the simulation.

The report was written throughout the sequence of steps mentioned above and was completed and reviewed at the end.

1.6 Report Outline

A brief overview of each chapter in the report is provided here. It acts as a primer for the reader and the identification of sections that may interest the reader more.

Chapter 2 explains the system concepts that is refered to throughout the report. It contains the mathematical derivation of the robotic gymnast and the simulated model. The system parameters with system identification tests are shown and demonstrates the simulated model is an acceptable representation of the physical model.

Chapter 3 describes the controller architecture to the swinging and balancing of the robotic gymnast. The specification for the controllers and the simulated responses of the controller are provided.

Chapter 4 contains the designs of the mechanical and electronic systems of the project. The various components used in the designs are discussed and explained.

Chapter 5 describes the software implemented to provide the report with these results. It explains the architecture of the software and the various functions implemented.

Chapter 6 provides the practical results of the controllers explained in chapter 3 and hypothesise unexpected behaviour in the experiments.

Chapter 7 concludes the report with a summary of the report and recommendation for future endeavours on the Feedback Control of a Robotic Gymnast.

Chapter 2

Conceptualisation and Modelling

[provide an overview]

2.1 System Concepts

The report contains many variable names and use of terminology for concepts that is used throughout the report. These variables and terminologies are defined here.

The double pendulum is a underactuated system which is defined as a system where the input to the system cannot command all of the state variables an instantaneous acceleration Tedrake. This is due to the control input only actuating the lower pendulum and the energy in the lower pendulum must be transferred to the upper pendulum to initiate an acceleration.

The robotic gymnast is described as a double pendulum consisting out of an actuated- and unactuated pendulum as seen in Figure 2.1. The position of the unactuated pendulum is described by the angle θ whereas the actuated pendulum is described by ϕ relative to θ. The angle's θ and ϕ are the independent parameters that describe the entire system.

There are two position of interest where the system contain special characteristics. These 2 positions are the stable- and unstable equilibrium positions. In the stable position the system is at rest hanging downwards where both θ and $\phi = 0\,\mathrm{rad}$. It is stable due to the system containing negative real poles resulting in the system returning to this position when disturbed. The unstable equilibrium position is where $\theta = 2\pi\,\mathrm{rad}$ and $\phi = 0\,\mathrm{rad}$ resulting in the robotic gymnast balancing in the inverted position. In this position the system contains positive real poles and any disturbance will cause the system to grow away from this position.

2.2 Mathematical Model

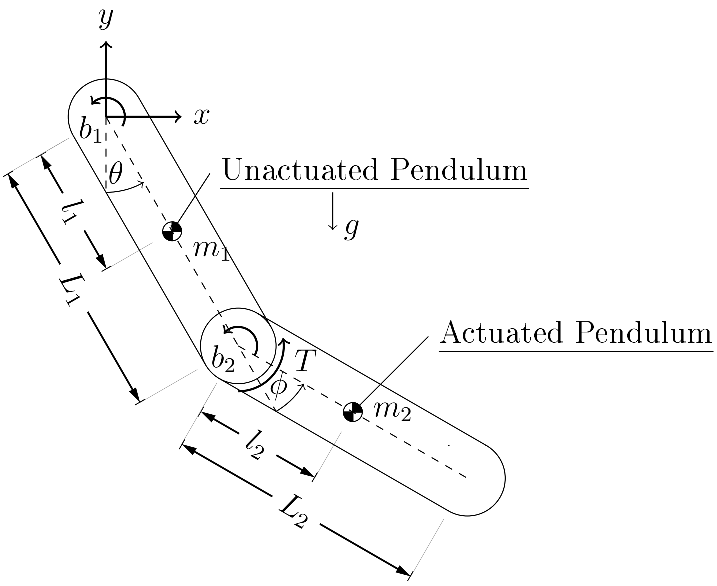

Figure 2.1: Free Body Diagram of the Double Pendulum

The approach taken to derive the mathematical model of the robotic gymnast is presented in this section. It is presented to allow the reader to understand parameters used throughout the report and critical to the implementation of the swing-up controller. The swinging of the robotic gymnast consists of non-linear behaviour and is required to fully derive the dynamics of the system. The detailed mathematical derivations are available in Appendix A.1. A summary of the motivation and paradigm approach to the derivation is provided here.

Figure 2.1 shows the free body diagram of the robotic gymnast which was modelled as two pendulums connected together with a hinge. Each pendulum was modelled as having their mass distributed arbitrary along their axis. A torque is actuating the lower pendulum and friction was modelled as a function of the angular velocity.

The Euler-Lagrange equation shown in (2.1) was used to derive the dynamics of the system by analysing the energy of the system which is easily defined as the potential energy T and the kinetic energy V of the 2 pendulums.

$$\frac{d}{dt}\frac{\partial \mathcal{L}}{\partial \dot{\vec{q}}} - \frac{\partial \mathcal{L}}{\partial \vec{q}} = 0 \tag{2.1}$$

$$\mathcal{L} = T - V \tag{2.2}$$

Using the Euler-Lagrange equation leads to the condense equations shown in (2.3) and (2.4),

$$d_{11}\ddot{\theta} + d_{12}\ddot{\phi} + h_1 + \psi_1 = 0 \tag{2.3}$$

$$d_{21}\ddot{\theta} + d_{22}\ddot{\phi} + h_2 + \psi_2 = \tau \tag{2.4}$$

where the coefficients are defined as

$$d_{11} = I_a + I_b + m_2(L_1^2 + l_2^2 + 2L_1 l_2 \cos(\phi)) \tag{2.5}$$

$$d_{12} = I_b + m_2(l_2^2 L_1 l_2 \cos(\phi)) \tag{2.6}$$

$$h_1 = -m_2 L_1 l_2 \sin(\phi)\dot{\phi}^2 - 2m_2 L_1 l_2 \sin(\phi)\dot{\phi}\dot{\theta} \tag{2.7}$$

$$\psi_1 = (m_2 l_1 + m_2 L_1) g \cos(\theta) + m_2 l_2 g \cos(\theta + \phi) + f_{c_1} \tag{2.8}$$

$$d_{21} = I_b + m_2(l_2^2 + L_1 l_2 \cos(\phi)) \tag{2.9}$$

$$d_{22} = I_b + m_2 l_2^2 \tag{2.10}$$

$$h_2 = m_2 L_1 l_2 \sin(\phi)\dot{\theta}^2 \tag{2.11}$$

$$\psi_2 = m_2 l_2 g \cos(\theta + \phi) + f_{c_2} \tag{2.12}$$

The friction that develops in the pendulums are for now represented by the f_{c_1} and f_{c_2} terms and will be expanded in the system identification section.

2.3 Simulation Model

The mathematical model derived in the previous section was implemented in a simulation program so that the controllers can be tested in simulation. Simulating the model allows the designer to understand how system parameters influence the dynamics of the system and the verification of controllers implemented. It will be presented by discussing the non-linearities added to represent the physical model better.

Simulation of the robotic gymnast was done using *MATLAB Simulink*. The differential equations shown in equation (2.3) and (2.4) were implemented using the *MATLAB Function* box. It was required to write $\ddot{\phi}$ and $\ddot{\theta}$ as the subject in each of the *MATLAB Function* box to allow MATLAB to simulate the model.

Non-linear behaviour introduced by sensors and components were added such as saturation of the motor torque, gearbox backlash and quantisation of sensory data. These non-linearities were implemented to allow the simulation to be an acceptable representation of the physical system. The Simulink Model used for simulation is shown in Figure 2.2.

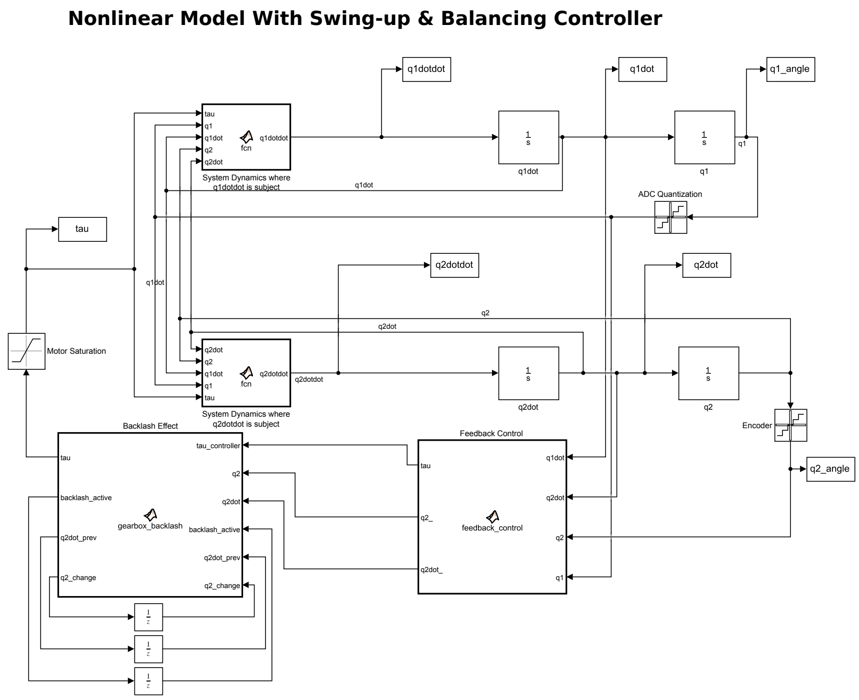

Figure 2.2: MATLAB Simulink Model

2.4 System Identification

The system identification tests are done to determine the characteristics that describe the behaviour of the system. These characteristics include the damping ratio's and natural frequencies of the system. These characteristics will be presented by showing measured responses and how these responses can be modelled.

The project started off with a previous physical model which provided realistic system parameters to allow the simulation to be an acceptable representation of a physical model. From using these previous system parameters the simulation provided a set of specifications for the new mechanical design. All responses shown and values calculated are based on the new mechanical design parameters shown in Table 2.1.

The system is described by two independent parameters and is expected to contain two natural frequencies each accompanied by a damping coefficient. The first natural frequency of the system was determined by inspecting the response of the system when starting at an initial condition and keeping $\phi = 0\,\mathrm{rad}$ throughout the response. This was done by using a lightweight PVC pipe that has negligible effect on the weight of the system. The actuated pendulum and unactuated pendulum are constrained to this pipe to ensure the two pendulums stay in-line with each other and thus ensuring $\phi = 0\,\mathrm{rad}$. The

System Parameter	Value
L_1	$0.235\,\mathrm{m}$
L_2	$0.314\,\mathrm{m}$
I_A	$0.0022\,\mathrm{kg}\cdot\mathrm{m}^2$
I_B	$0.0054\,\mathrm{kg}\cdot\mathrm{m}^2$
m_1	$0.576\,\mathrm{kg}$
m_2	$0.492\,\mathrm{kg}$
l_1	$0.205\,\mathrm{m}$
l_2	$0.238\,\mathrm{m}$

Table 2.1: System Parameters

response of the system is shown in Figure 2.3 starting at an initial condition of roughly $\theta = \frac{\pi}{6}$. The accuracy of the initial conditions is of little importance, but must allow the response to contain a few oscillations to accurately determine the parameter of interest.

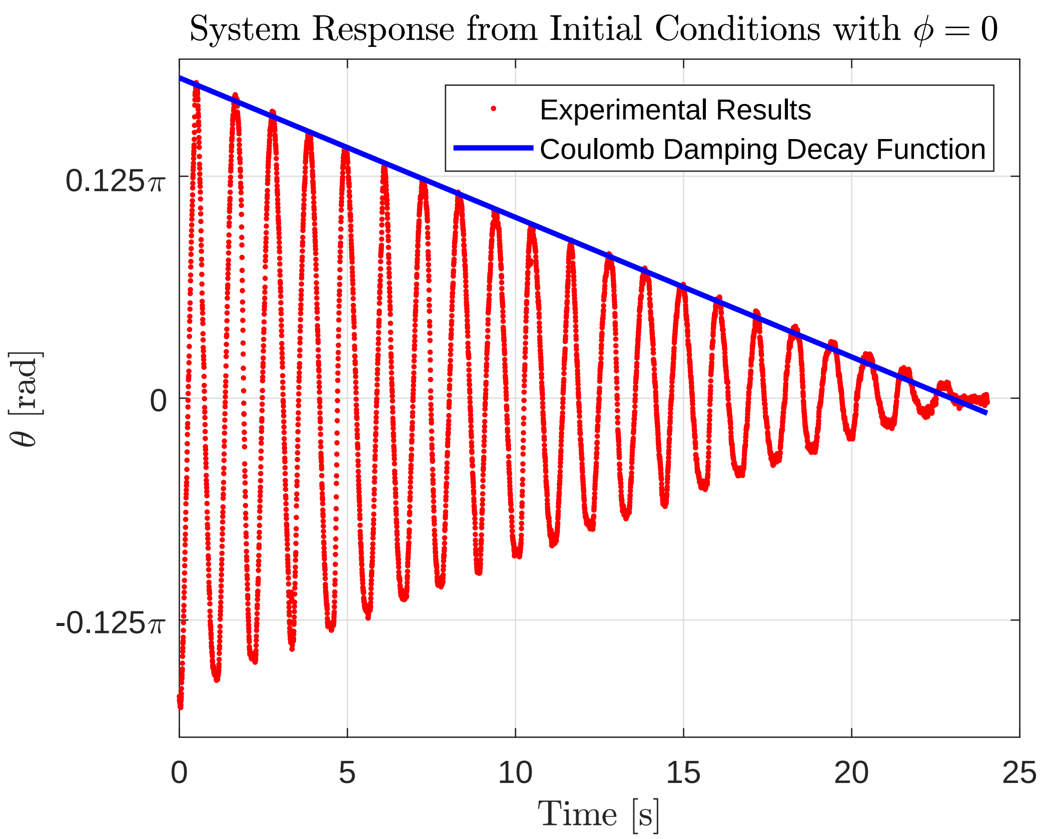

Figure 2.3: Initial Condition System Response while $\phi = 0\,\mathrm{rad}$

The second natural frequency was determined by analysing the response of the system when ϕ starts at an initial condition and keeping $\theta = 0\,\text{rad}$ throughout the response. This was accomplished by constraining the unactuated pendulum using hard stops. Figure 2.4 shows the measured response of the system when ϕ starts at an initial condition and keeping $\theta = 0\,\text{rad}$.

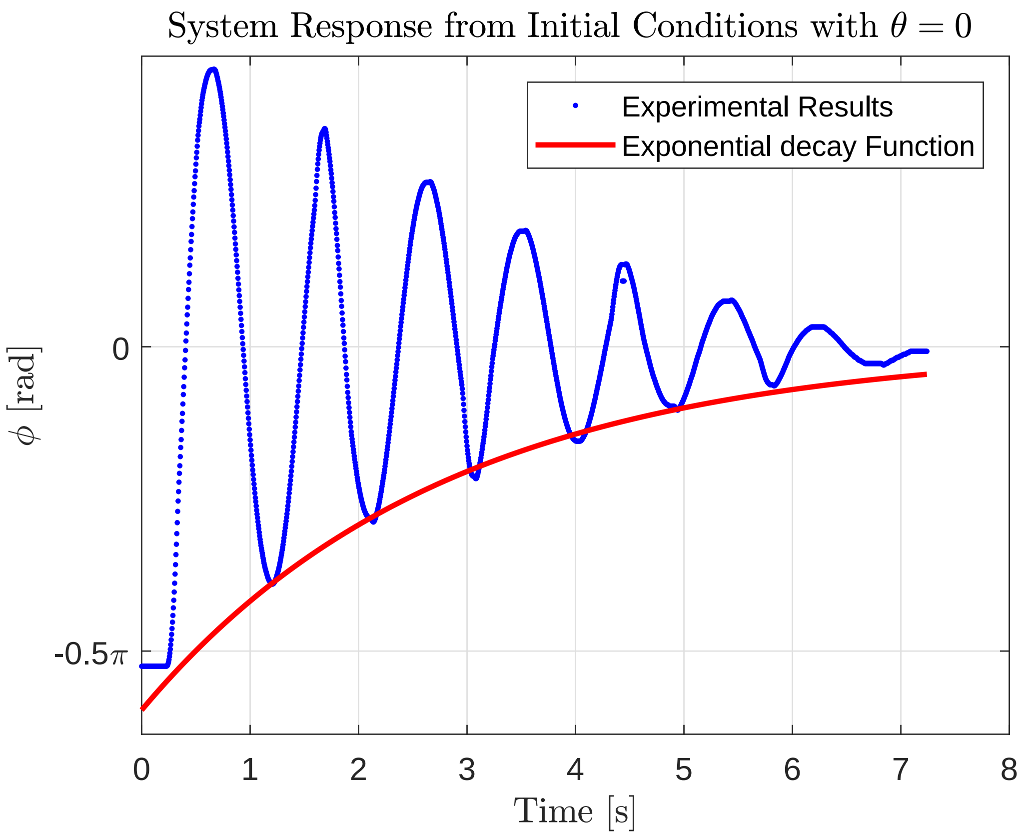

Figure 2.4: Initial Condition System Response while $\theta = 0\,\text{rad}$

The responses shown in Figure 2.3 and 2.4 can be characterised as equation (X) where the frequency of oscillation is caused by the damped natural frequency. This damped natural frequency was determined by measuring the time difference between peaks. The practical results contains a variation on the time difference between peaks and thus the mean of the time differences were calculated and shown in Table **??**.

The friction torques, f_{c_1} and f_{c_2} that were set as unknowns in the derivation of the robotic gymnast will be expanded on in the following section by analysing how the decaying of the responses can be characterised.

The response shown in Figure 2.3 is under the influence of coulomb damping due to the response being characterised by the amplitude decaying linearly with a constant slope. Coulomb damping is caused by sliding friction and its torque is opposite to the direction of rotation (Inman, 2015). It is thus characterised as

$$f_{c_1} = \left\{ \begin{array}{cc} -\mu N & \dot{\theta} > 0 \\ 0 & \dot{\theta} = 0 \\ \mu N & \dot{\theta} < 0 \end{array} \right\}$$

It is shown in Inman (2015) that the slope is defined as

$$-\frac{2\mu N \omega_n}{\pi m g} \tag{2.13}$$

where N is the normal force. The slope seen in the decay function in Figure 2.3 was calculated using linear regression and by knowing the terms in equation (2.13) the combined μN term can be calculated as shown in Table **??**.

The response shown in Figure 2.4 is under the influence of viscous damping due to the amplitude decaying exponentially with time and this behaviour is modelled by the following equation:

$$\tau(t) = Ae^{-\zeta \omega_n t}$$

where ω_n is the natural frequency, ζ the damping ratio of the system and A represents the initial amplitude. The damped natural frequencies of the system have already been determined and linear regression was used to determine the best ζ that will fit the measured data. The decaying function is shown in Figure 2.4 with the ζ value shown in Table **??**. It is visible from the response that the damping ratio fits the data well and only starts to deviate near steady state.

The damping moment, f_{c_2} that develops between the stator and rotor of the hinge can then be characterised as $2\zeta\omega_n(\dot{\phi} - \dot{\theta})$. The subtraction of $\dot{\theta}$ is due to the rotor of the hinge rotating relative to the stator.

2.5 Model Validation

The model implemented in simulation must be able to describe the physical model to an acceptable degree to allow any further developments on the simulated model. The simulated model will be validated by comparing the experimental system characteristic values to those attained in simulation.

Table 2.2 shows the experimental values determined in the previous section against the simulation characteristic and indicates the simulation model

System	ω_{n_1}	ω_{n_2}	ζ_1	ζ_2
Experimental	5.692	6.793		
Simulation	5.654	6.704		

Table 2.2: Experimental Characteristics vs Simulation Model Characteristic

represents the physical model well.

Figure 2.5 and 2.6 provides a visual verification of which the damping effects are modelled to an acceptable degree. It is visible that the simulated response fits the experimental response well, matching the frequency of oscillation during high velocities and large angles. It is only near steady state where the simulated responses deviates a little.

Figure 2.6 does not describe the damping effect throughout the entire response. This is expected due to the damping force not being constant throughout the response as seen in Figure 2.4. The average of the damping coefficients were selected and results in variances.

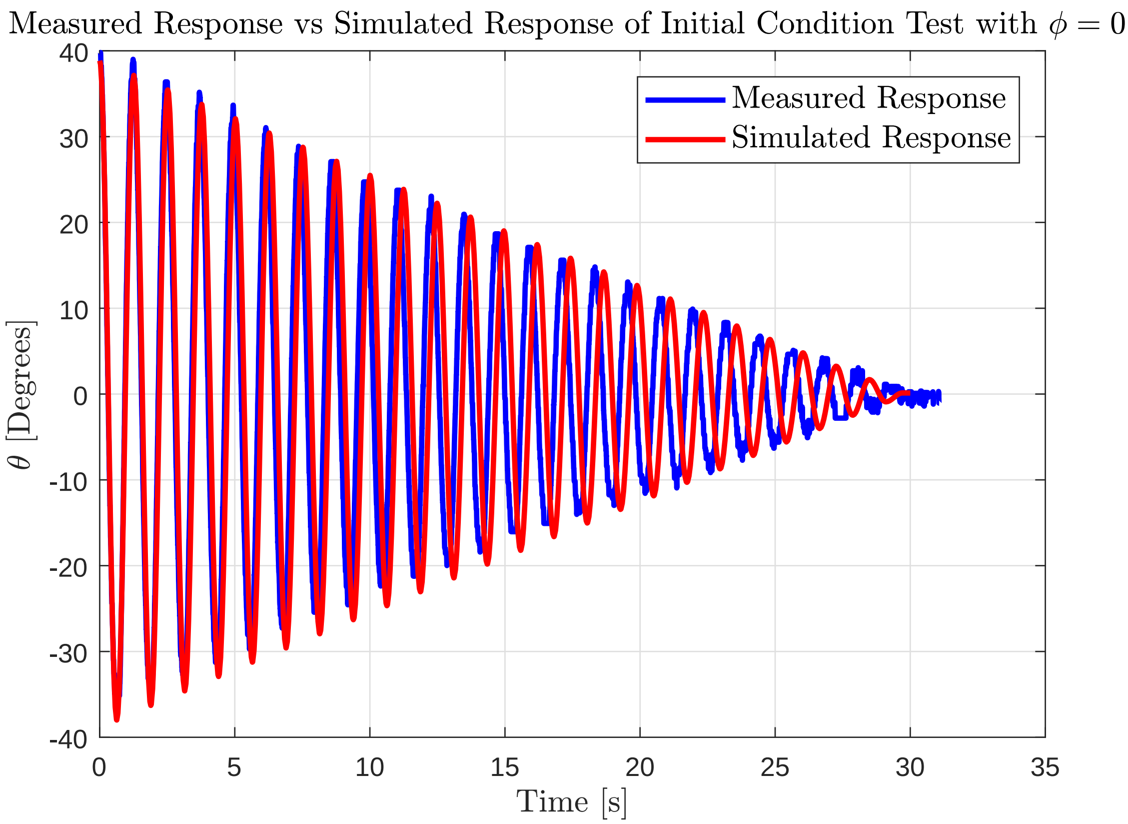

Figure 2.5: Comparison between Simulated and Measured Response with $\phi = 0\,\mathrm{rad}$ throughout

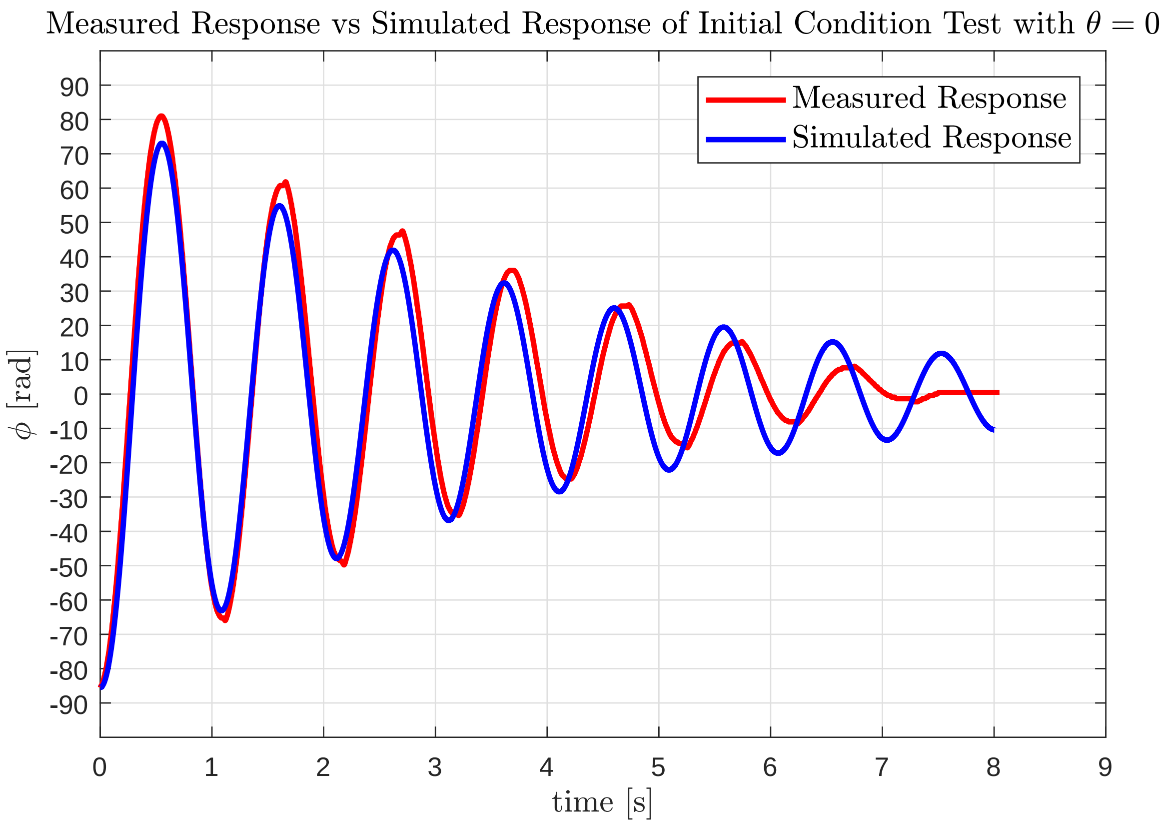

Figure 2.6: Comparison between Simulated and Measured Response with $\theta = 0\,\mathrm{rad}$ throughout

Chapter 3

Feedback Control Design

This chapter presents the design of the feedback control laws to swing up and balance the robotic gymnast. Two separate controllers are used, one to swing up the robotic gymnast from the hanging position to the vertical position, and another to catch and balance the robotic gymnast when it reaches the inverted position. The design of the balancing controller will be presented first, followed by the design of the swing up controller. The chapter will conclude with a simulation that illustrates the integrated swing up and balancing of the system, starting with the swing up controller and switching over to the balancing controller.

3.1 Balancing Controller

Provided the robotic gymnast is in the vicinity of the unstable equilibrium position, a balancing controller is required to balance the system in the inverted position. The design approach was based on the premise that the swing-up controller will swing the robotic gymnast to the vicinity of the unstable equilibrium position where the balancing controller will take over. This section will focus on the aspects required to implement this balancing controller.

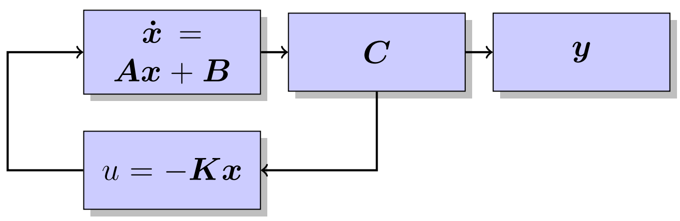

Figure 3.1: State Space Representation of the Balancing Controller

3.1.1 Controller Architecture

Figure 3.1 shows the block diagram that implements the balancing controller, and it is clear that the state space representation of the system was used. This requires the system to be a linear time invariant (LTI) system, but the system described in equation (2.3) and (2.4) are not linear. This requirement was satisfied by linearising the system.

Another aspect of the balancing controller is that there are no reference input to instruct the controller to guide the robotic gymnast to the unstable equilibrium position. The linearised system at the inverted position is unstable. The feedback control makes the close loop system stable around the inverted state that would normally be unstable for the uncontrolled system.

3.1.2 Requirements/Specifications and Constraints

The independent parameters, ϕ and θ, will be condensed from now on as a vector describes as

$$\vec{q} = \begin{bmatrix} \theta \\ \phi \end{bmatrix}$$

The requirements set out for the balancing controller were to bring the robotic gymnast to the unstable equilibrium position from an initial condition range of:

$$\vec{q_i} = \left\{ \begin{array}{c} \theta \in [177°, 183°] \\ \phi \in [-5°, 5°] \end{array} \right\}$$

The response must have a settling time of 1 seconds and a percentage overshoot M_p of 10%.

These requirements were selected to give the swing-up controller enough margin to bring the system to the vicinity of the unstable equilibrium position where the balancing controller is capable of balancing.

3.1.3 Plant Linearisation

As mentioned previously, to implement the state space representation the system must be a LTI system. This was achieved by using the Taylor Series Expansion to linearise the system at the unstable equilibrium position.

The system is linearised at

$$[\vec{q_s}, \dot{\vec{q_s}}, \ddot{\vec{q_s}}]^T = [\pi, 0, 0, 0, 0, 0]$$

with the mathematical details shown in Appendix A.2. This linearised model can then be written in the state space form to implement a feedback gain. The state space variables are chosen as $\Delta\vec{q}$ and $\Delta\dot{\vec{q}}$ which results in the state space representation as:

$$\dot{\vec{q}} = \boldsymbol{A}\Delta\vec{q} + \boldsymbol{B}u$$
$$\vec{y} = \boldsymbol{D}\Delta\vec{q} + \boldsymbol{0}u$$

The poles of the system are identified by determining the eigenvalues of the $\boldsymbol{A}$ matrix. The linearised system remains a coupled system which results that the quadratic eigenvalue problem shown in equation (3.1) was required to be solved to identify the poles. The solved quadratic eigenvalue problem results in the following eigenvalues using the system parameters in Table 2.1.

$$Q(\lambda) = \lambda^2 M + \lambda C + K \tag{3.1}$$

$$\vec{s} = \begin{bmatrix} -12.06 \\ -5.05 \\ 10.64 \\ 5.01 \end{bmatrix}$$

The eigenvalues of the system are all real indicating the response of the system when disturbed is an exponential function. This can be explained by realising the linearised system is modelled as a single pendulum. Once the single pendulum is disturbed from the unstable equilibrium position it would continue to rotate downwards and not with an oscillatory response.

3.1.4 Full State Feedback Design

The poles of the system are pairs of positive and negative real poles that indicate an unstable system. This is expected due to the system being linearised at the unstable equilibrium position. When the linearised system is at rest, any disturbance will result in a theoretically infinite growth of the state variables, but this behaviour can be controlled by introducing feedback.

These poles will be moved to the desired position by using the method of dominant poles. The method of dominate poles chooses a pair of the poles for the closed-loop system and select the other open-loop poles to have real parts with much larger natural frequencies. This allows the higher-order system response to be characterised as a second-order response (Gene F. Franklin, 2015).

Assuming a second order system and using the requirements defined, the pole locations can be calculated using equation (3.2) and (3.3)

$$M_p = \exp\left(\frac{-\pi\zeta}{\sqrt{1-\zeta^2}}\right) \tag{3.2}$$

$$t_s = \frac{4.6}{\zeta\omega_n} \tag{3.3}$$

and knowing the poles are described seen in equation (3.4)

$$p = \zeta\omega_n \pm j\omega_d \tag{3.4}$$

results in the desired pole locations as:

$$\vec{p} = \begin{bmatrix} -4.6 + j6.13 \\ -4.6 - j6.13 \\ -23 \\ -23 \end{bmatrix}$$

3.1.5 Simulation Response

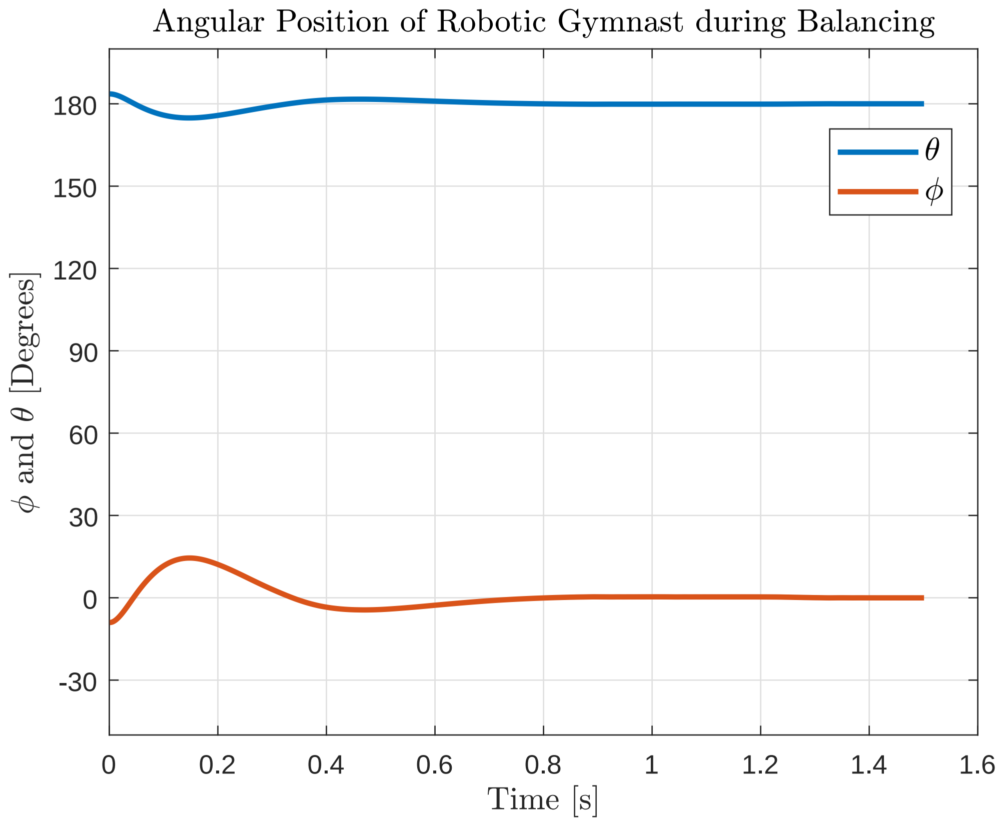

Figure 3.2: Balancing of the Robotic Gymnast

Figure 3.2 shows the robotic gymnast balancing around the unstable equilibrium position from an initial condition of

$$\vec{q}_i = \begin{bmatrix} 183.6° \\ -9° \end{bmatrix}$$

The response shows that the controller meets the requirement of balancing the robotic gymnast from required initial condition and reaches steady state within 1 seconds. The overshoot requirement of 10% has also been achieved on the unactuated pendulum.

The identified coulomb damping that the unactuated pendulum experience is not possible to linearised (ref). This friction was approximated as viscous damping in the linear model and was acceptable due to the physical model showing characteristic of viscous damping near steady state visible in Figure 2.3.

3.2 Swingup Controller

For the robotic gymnast to swing from the stable equilibrium position to the unstable equilibrium position the feedback control must deal with the nonlinearities of the system.The design approach, including how the feedback controller handles the nonlinearities, is explained in the following section.

3.2.1 Controller Architecture

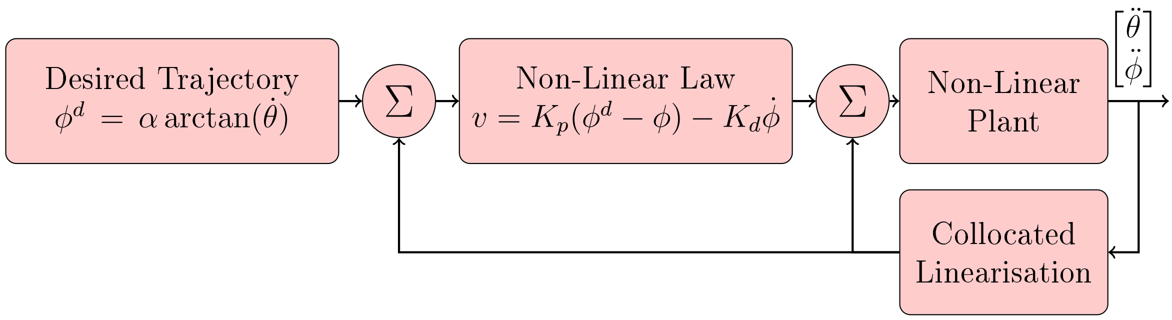

Figure 3.3: Block Diagram of the Non-Linear Controller

Figure 3.3 shows a high-level block diagram of the multiple parts of the swing-up controller. These parts are required to work in unison to allow the robotic gymnast to swing.

The collocated linearisation block linearises the response from the motor torque input to the actuated pendulum angle output. The linear control law controls the angle of the actuated pendulum ϕ to follow a command reference angle ϕ^d. The controller gains Kp and Kd are designed to provide a good transient response. The swing up trajectory generator implements a nonlinear control law that provides reference commands ϕ^3 for the actuated pendulum angle ϕ, as a function of the angular rate $\dot{\theta}$ of the unactuated pendulum. The maximum angle command for the actuated pendulum is limited by the arctan function and the constant parameter α.

The swing-up controller implements classical control theory approach where gains are selected to characterise the response of the system based on the error of the desired trajectory and the actual trajectory of the system.

Each of the blocks shown in the block diagram will be discussed in the section below.

3.2.2 Requirements/Specifications and Constraints

The requirements of the swing-up controller is to swing the robotic gymnast upwards under 30 seconds in the vicinity of the unstable equilibrium position. The vicinity of the unstable equilibrium position is defined as $\theta = 2\pi\,\mathrm{rad} \pm \frac{\pi}{30}$ and $\phi \in [-5°, 5°]$.

The constraint placed on the swing up controller is that its torque command to the motor actuator should not exceed 50% of the stall torque of the motor.

The first requirement is to provide a feasible solution to the swing-up of the robotic gymnast and allow the swing-up sequence to be captivating. The second requirement is to ensure the linear approximation of the system is acceptable when the balancing controller is active to bring the system to the inverted position and balance. The constraint placed was to increase the safety in testing and prolonging the life of the motor.

3.2.3 Feedback Linearisation

Murray and Hauser (1991) showed that it is not possible to linearise the dynamics of the robotic gymnast using static state feedback and non-linear transformation, but that it is possible to achieve a linear response from one of the outputs of the system (either the actuated or the unactuated pendulum angle) using nonlinear feedback that provides partial feedback linearisation.

Collocated linearisation is a form of partial feedback linearisation where a non-linear control input τ is used to linearise the response of the actuated pendulum $\ddot{\phi}$. By analysing equation (2.4), the input τ was chosen to cancel all the non-linearities of the system and add an additional outer loop control input v_2 as seen in equation (3.5). This results in the unactuated pendulum to see a indirect force and the problem can be reduced to finding the outer loop control input to force the actuated pendulum to swing upwards (Spong, 1995).

The final result of the collocated linearisation is shown below, and the complete derivation can be found in Appendix ??.

$$\tau = d_{21}\ddot{\theta} + v_2 d_{22}\ddot{\phi} + h_2 + \psi_2 \tag{3.5}$$

$$d_{11}\ddot{\theta} + h_1 + \psi_1 = -d_{12}v_2 \approx F \tag{3.6}$$

$$\ddot{\phi} = v_2 \tag{3.7}$$

The subtle practical implication of using collocated linearisation is that the system being controlled must be well defined. If this is not the case the non-linear input τ will introduce other unwanted dynamics that could lead to undesirable behaviour.

3.2.4 Nonlinear Control Law

The ability to control the actuated pendulum to follow a desired trajectory, provides the possibility to increase the energy of the system if the correct trajectory is chosen. The increase of energy in the system will cause the pendulums to rise from their stable equilibrium position and start swinging upwards. The desired trajectory for ϕ was chosen as equation (3.8) determined by Spong.

$$\phi^d = \alpha \arctan(\dot{\theta}) \tag{3.8}$$

This desired trajectory was derived by analysing a single pendulum and approximating the force it experiences as seen in equation (3.6). By using this approximation Spong showed that the desired trajectory will increase the energy in the system. The desired trajectory also tries to allow the actuated pendulum to swing in phase with the non-actuated pendulum and by this approach the energy of the actuated pendulum is transferred to the unactuated pendulum (Spong, 1995).

The outer loop control input, v_2, then implements the classical control approach where gains are selected to characterise the response of the system based on the error seen in equation (3.9).

$$v_2 = K_p(\phi^d - \phi) - K_d\dot{\phi} \tag{3.9}$$

The coefficient α used in equation (3.8) constrains the actuated pendulum to stay within a interval of $\phi \in [-\beta, \beta]$ where $\alpha < \beta$ (Spong, 1995). This provides better control over the system to stay within the null controllability region when the system reaches the unstable equilibrium position.

Another side-effect of using the non-linear controller is that at rest the system will not start to swing-up. At rest, the conditions are: $\phi = 0\,\text{rad}$ and $\dot{\phi} = 0\,\text{rad/s}$, and results in the control output seen in equation (3.9) to be zero. This effect was overcome by giving the system a small initial condition to start the swing-up controller.

Gain Constant	Value
K_p	58
K_d	14

Table 3.1: Gain Constant used during Simulation

3.2.5 Simulation Response

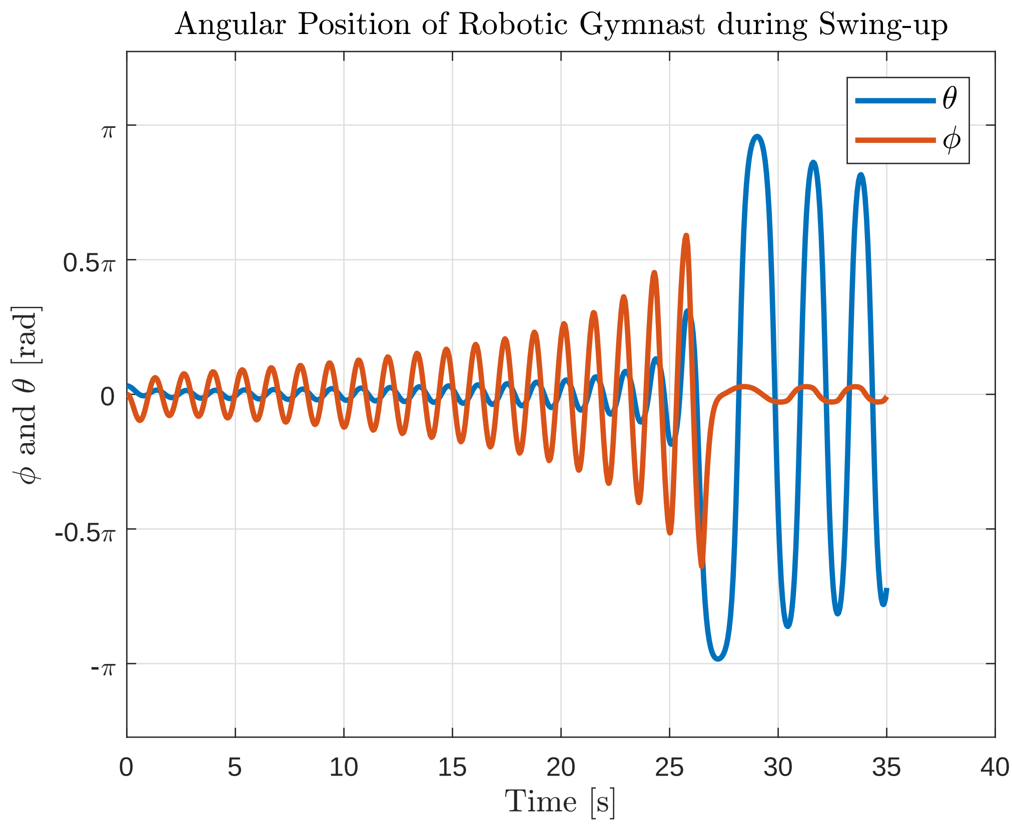

Figure 3.4: Swing-up of the Robotic Gymnast

Figure 3.4 shows the swing-up controller swinging the robotic gymnast from the stable equilibrium position to the vicinity of the unstable equilibrium position with gain constants used shown in Table 3.1. There are a few interesting occurences in the responses mentioned in the previous section which needs to be brought to the attention of the reader.

Firstly the robotic gymnast is required to start at an initial condition for the swing-up control law to be active and this is seen with θ starting at 11°. Secondly, the amplitude of ϕ is seen to decrease suddenly when the system nears the inverted position. This is due to α being reduced when the robotic gymnast nears the inverted position.

The response shows the swing-up controller meets the designed requirements by swinging the robotic gymnast to the vicinity of the unstable equilibrium within 30 seconds and θ and ϕ are in the designed region for the balancing controller to bring the system to the inverted position.

3.3 Simulation Results

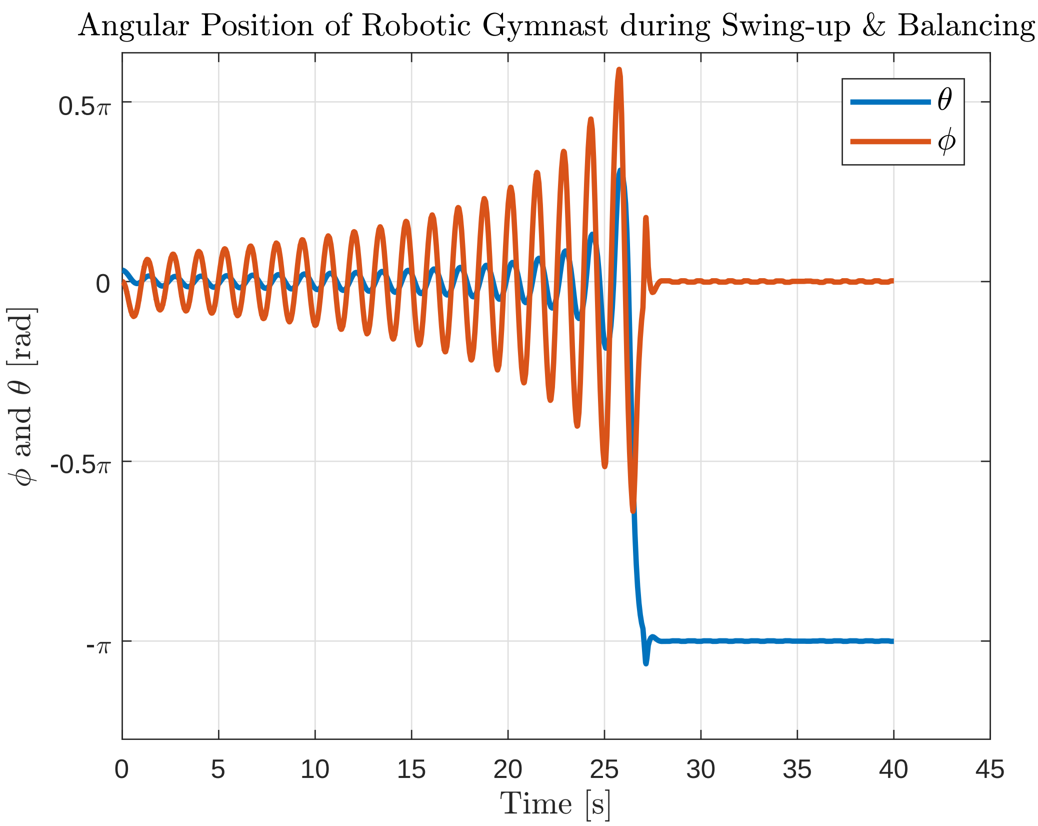

Figure 3.5: The Swing-Up & Balancing of the Robotic Gymnast

Once both controllers were capable of meeting the requirements set out, they needed to be combined to achieve the swing-up and balancing of the robotic gymnast. Figure 3.5 shows the response of both controllers combined that achieved the swing-up and balancing.

During the swing-up the α value was reduced as the robotic gymnast started nearing the unstable equilibrium position as seen below.

$$\alpha = \left\{ \begin{array}{cc} \frac{\pi}{2} & \frac{-\pi}{2} < \theta < \frac{\pi}{2} \\ \frac{\pi}{12} & \\ \frac{\pi}{24} & \frac{-\pi}{1.1} > \theta\theta > \frac{\pi}{1.1} \end{array} \right\}$$

Chapter 4

Hardware Design and Implementation

This chapter presents the design and implementation of the physical gymnastic robot that was used to practically demonstrated the feedback control system. The design and implementation of the mechanical hardware is presented first, followed by the design of the electronic hardware. The chapter concludes with the tests that were performed to verify that the electronic hardware interfaces correctly with the motor driver and the two angle sensors.

4.1 Mechanical Hardware

The mechanical system was designed to practically demonstrate the feedback controllers to swing and balance the robotic gymnast. The mechanical system will be presented by discussing the various components required to be implemented, mechanical characteristics and a force analysis.

It is important that the physical model holds the assumption made during the derivation of the robotic gymnast. These assumptions include planar dynamics of the robotic gymnast and rigid body dynamics. The assumption of rigid body dynamics were easily met due to the forces acting on the pendulums results in negligible strain and thus elongation can be ignored. The assumption of planar dynamics comes in affect with the connection between the rotating shaft and the unactuated pendulum. If the assumption holds there should be no vibration of the pendulum in any other direction than the rotating plane. This assumption holds in the mechanical system due to four screws used to keep the unactuated pendulum perpendicular to the shaft.

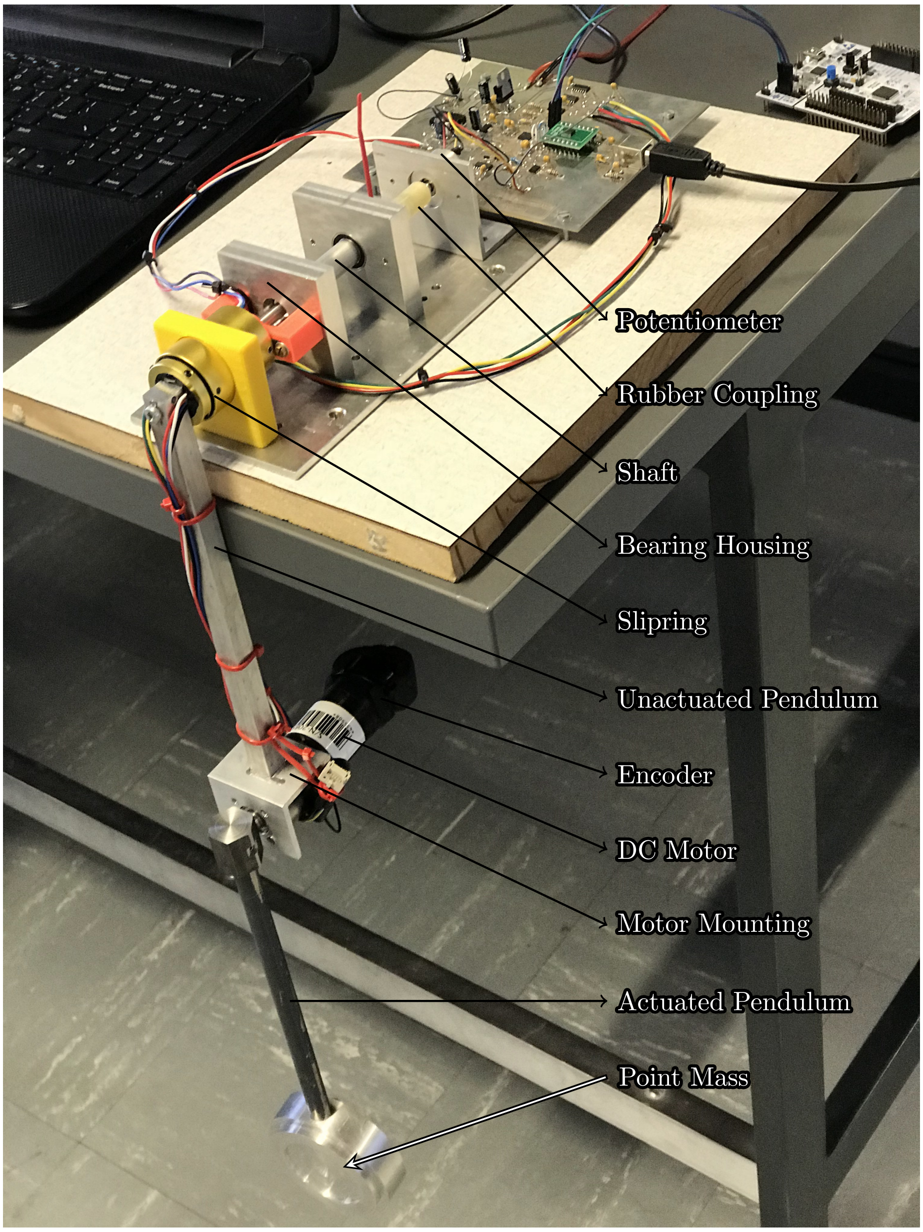

Figure 4.1: PCB

4.1.1 Assembly

Figure 4.1 emphasises important components that are discussed in the following section and explains their significance of use.

The electrical slipring converts the rotating wires that leads to the motor mounted on the unactuated pendulum to stationary wires allowing for free rotation and easy connection to the electrical design.

The bearing housing holds the ball-bearings in place ensuring for no vibration and misalignment. These ballbearings were press-fitted into the housing, ensuring a secure connection.

The potentiometer's shaft is connected to the shaft by means of a rubber tube. The rubber tube was chosen was chosen as it easily connects and allows for misalignment. The delay of measurement due to elasticity of the rubber is negligible due to the system experiencing low acceleration.

4.1.2 Structural Force Analysis

The stress analysis of the rotating shaft is presented to provide the reader confidence in the shaft design. It will be presented by calculating the static yield safety factor and discussing whether the safety factor is sufficient.

The shaft was analysed as a 3 point supported beam shown in Figure 4.2 with a constant diameter throughout, using the smallest diameter in the design. The forces acting on the beam is the torque T due to the rotating pendulums, and the normal force F due the centripetal force of rotation and weight of the pendulums.

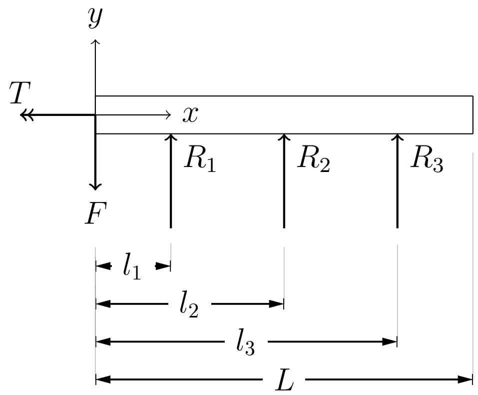

Figure 4.2: Model of Rotating Shaft as a Simplified Beam

The beam is a static undetermined beam and was solved using the principle of superposition and results in the reaction forces shown in equations (4.1), (4.2) and (4.3).

$$R_1 = 100\,\mathrm{N} \tag{4.1}$$

$$R_2 = \frac{8Fl_1[l_3^2 - l_2^2]}{l_3[4l_2^2 - 3l_3^2]} = 90\,\mathrm{N} \tag{4.2}$$

Stresses	$x = 0.1\,\mathrm{m}$	$x = 0.25\,\mathrm{m}$
σ_{f_1}	5	
σ_{f_2}	3.3	
σ_{f_3}	3.3	
τ_f	12	
M_{max}	12	

Table 4.1: Stresses developed in Shaft

$$R_3 = 33\,\mathrm{N} \tag{4.3}$$

The maximum bending stress occurs at $x = 0.1\,\mathrm{m}$ and the maximum torsion stress at $x = 0.25\,\mathrm{m}$. The safety factor of yielding will be determined at these two positions.

Equations (4.5) and (4.4) are used to determine the maximum stresses at these two points and using the Mohor circle the principle stresses are determined. These stresses are shown in Table 4.1.

The conservative Von Mises theory shown in equation (4.6) was used to determine the safety factor on static yielding, where S_y is the yield stress of extruded aluminium. A safety factor on static yielding of 2 was determined. This is acceptable and indicates the shaft is capable of withstanding the load.

Fatigue due to cyclic loads were ignored due the shaft not rotating more than a 1000 times and the safety factor on static yielding on a conservative model is sufficient.

$$\sigma_f = \frac{M \cdot r}{I} \tag{4.4}$$

$$\tau_f = \frac{T \cdot r}{J} + \frac{F_{max}}{22} \tag{4.5}$$

$$n_s = \frac{S_y}{\sqrt{\frac{(\sigma_{f_1} - \sigma_{f_2})^2 + (\sigma_{f_2} - \sigma_{f_3})^2 + (\sigma_{f_3} - \sigma_{f_1})^2}{2}}} \tag{4.6}$$

4.1.3 Inertia of Pendulums

Figure 4.3 shows a functional drawing of the physical in order to aid the reader visually in understanding how the inertia of the system was determined. In equation (2.3) and (2.4) the I_a and I_b represents the inertia of the unactuated and actuated pendulum about the axis coming out of the page passing through their center of mass respectively.

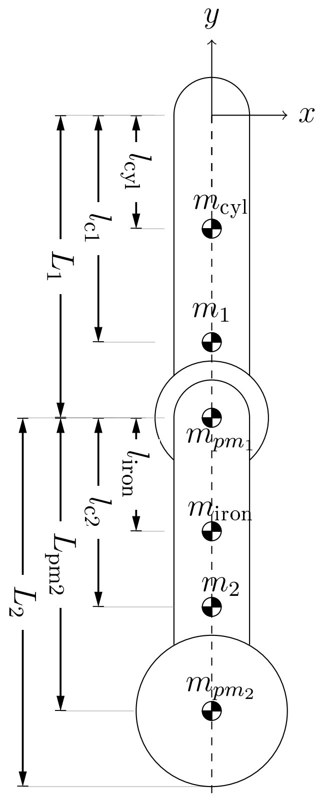

Figure 4.3: Simplified Drawing of Physical Model

Each pendulum contains parts that contribute to the pendulum's inertia due to each part representing a different physical form. How the inertia values shown in Table 2.1 were determined will be shown below with the physical system parameters shown in the Table 4.2

The actuated pendulum consist out of an aluminium square rod connected to the shaft and the motor mounting. The inertia of a square rod through it's center of mass is:

$$I_{cyl} = \frac{1}{12} m_{cyl}[w^2 + L_1^2]$$

The motor, gearbox and the motor mount was viewed as a point mass. Its inertia around the center of mass of the unactuated pendulum is:

$$I_{pointmass_1} = m_{pointmass_1} \cdot [L_1 - l_{c1}]^2$$

The total inertia of the unactuated pendulum around its center of mass is :

$$I_a = I_{pointmass_1} + I_{cyl} + m_{cyl} \cdot [l_{c2} - l_{cyl}]^2$$

where the parallel axis theorem was used to move the aluminium rod's inertia to the center of mass of the unactuated pendulum.

Non-Actuated Pendulum	Value	Actuated Pendulum	Value
m_{cyl}	0.1443	m_{iron}	
w_{cyl}	3.3	w_{iron}	
$m_{\text{pointmass1}}$	0.4320 kg	$m_{\text{pointmass2}}$	
l_{cyl}	0.235 m	l_{iron}	
L_{c1}	0.235 m	L_{c2}	
L_1	12	L_2	

Table 4.2: Physical Model Paramaters

Pendulum	Center of Mass [m]
Unactuated	0.2056
Actuated	0.1940

Table 4.3: Center of Mass for Each Pendulum from their Rotating Hinge

The actuated pendulum contains similar parts as the unactuated pendulum: a pointmass at the bottom and an iron rod connected to the motor shaft. Determining the inertia of the actuated pendulum is thus exactly the same as the unactuated pendulum.

During the simulation it was noticed that the ratio between the unactuated and actuated pendulum $\frac{I_b}{I_a}$ should be 1 or greater for the swing-up controller to bring the robotic gymnast to the unstable equilibrium position in a feasible time frame. This is the reason adding another pointmass to the actuated pendulum to compensate for the inertia the motor creates.

4.1.4 Center of Mass

Each pendulum can be seen as a system containing discrete components, where each component center of mass is easily identified. Both iron rod and aluminium rod center of mass is in the middle of their rod lenght and the rest are seen as point masses. However each of these components center of mass contribute to the center of mass of each pendulum.

The center of mass for each pendulum from their hinge of rotation shown in Table 4.3 was calculated using equation (4.7).

$$\vec{r} = \frac{\sum_i^j r_i m_i}{\sum_i^j m_i} \tag{4.7}$$

4.1.5 Motor

The chosen motor used during experiments was the *Faulhaber DC 3257 012 CR* micromotor. It was used in combination with the *Faulhaber Planetary Gearhead 32/3* Series. The gearbox is a 2 stage reduction gearbox with an overall rounded reduction ratio of 14:1. The motor is capable of providing a stall torque of 539 mNm which is a converted output torque from the gearbox of 7.646 Nm.

The motor terminal connection is connected directly to the PCB of the electronic design being routed through the slipring. The motor assembly contains an encoder for position measurements and it's signal and power connection is also routed through the slipring and connected to the PCB.

4.2 Electronic Hardware

The electronic hardware was a crucial component for the successful implementation of the robotic gymnast. The electronic design provided the means to determine the system characteristics and verification of the simulated model. It will be presented by discussing the various components implemented to achieve the results in this report.

4.2.1 System Description

Figure 4.5 provides a system overview of how the different subsystems functions together and what inputs are outside from the PCB design.

The micro-controller receives the different signals that has been correctly conditioned from supporting circuitry to interpret the dynamics of the system. From these signals it is able to output the correct signals to instruct the next command.

The digital logic circuit that consist out of logic level converters acquires the signal from the microcontroller and performs signal conditioning to interface with the motor driver and determines the correct direction to rotate the motor.

The motor driver controls the DC brushed motor based of the digital signals and provides a proportional feedback current that is delivered to the unity-gain amplifier.

The motor contains an encoder that indicates the direction and position of the rotor through digital signals that is sent through a digital logic filter to

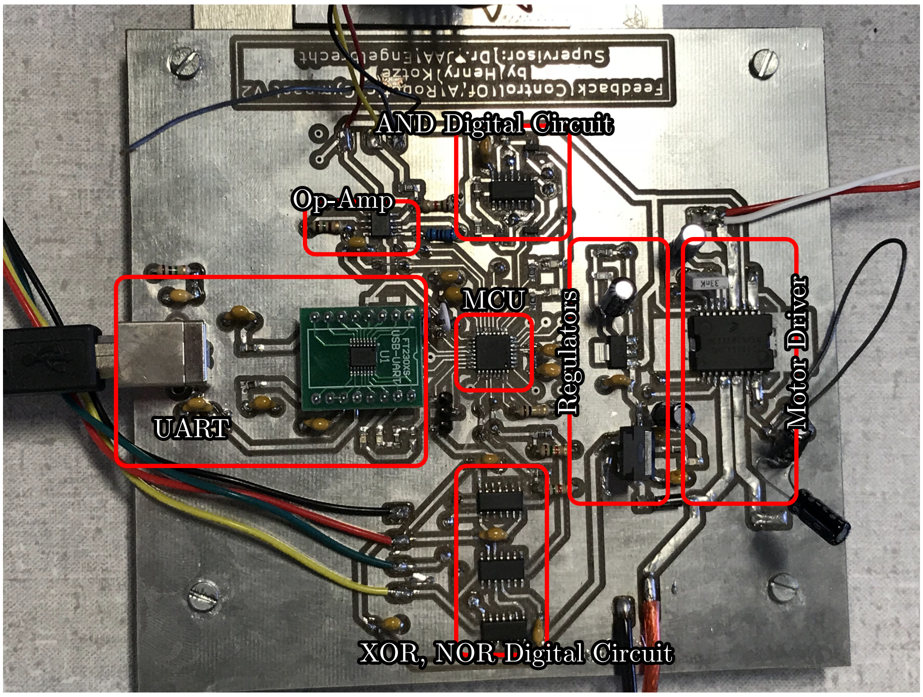

Figure 4.4: PCB

retrieve only critical information from the encoder signals.

The physical model contains a potentiometer that measures the unactuated pendulum's angle and this signal is sent to the unity-gain amplifier.

The microcontroller will use the UART interface as its data acquisition protocol to send the necessary information to the computer.

The micro-controller is programmed using the Serial Wire Debug (SWD) protocol to transfer the binaries from the computer.

Power is provided using a external 12V power-supply, which will provide power to the motor, but also using a regulator to down convert/step to a 5V and 3.3V to provide power to the microcontoller and the other peripherals.

4.2.2 Microcontroller

The microcontroller chosen is the STM32F030C6. The selection was done according to the ease of setting up, memory size, physical dimensions and the peripherals it provided. The selection is described below.

The STM32F030C6 is based on the ARM M0 architecture which is ARM's entry level microcontroller architecture. It requires little support circuitry to

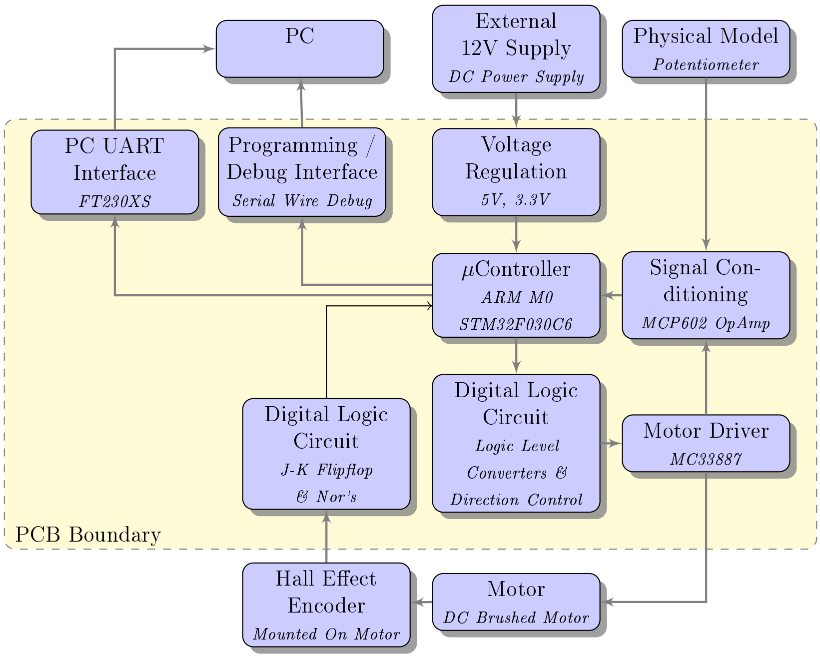

Figure 4.5: Electronic System Overview

have a microcontroller which is fully functioning with only the SWD protocol to program the chip.

It was difficult to determine the memory size specification for the project. This uncertainty ensured that the largest memory size the ARM M0 architecture could provide was selected.

The Electrical and Electronic Department's PCB manufacturing machine can only provide a minimum track width of 0.3 mm. This resulted in choosing a microcontroller which footprint would meet this requirement.

Based on the conceptual design, the chosen microcontroller was required to contain 2 ADC's channels, minimum of 5 GPIO's and 1 serial communication peripheral.

From these requirements and specification the STM32F030C6 was the best candidate to meet all of the above mentioned requirements..

4.2.2.1 Programming / Debug Interface

The *Atollic TrueSTUDIO for ARM 8.0.0* Integrated Development Environment (IDE) was used for writing the source code which converts the source code to the Executable and Linkable Format (.elf) file. These .elf files is then written using the SWD protocol to the microcontroller. Debugging of the

Component	Supply Voltage [V]
Digital Logic, Op-Amp & Sensors	5
Microcontroller	3.3
Motor Driver	12

Table 4.4: Suppy Voltage's for the different components

source code occurred using the same IDE which allows the programmer to inspect variables, timers and logic.

4.2.2.2 PC UART Interface

The purpose of the Universal Asynchronous Receive Transmit (UART) to serial communication was for the data acquisition of the system response, debugging and sending the control input that was computed on the external computer.

The external computer executed a Python script that was listening for any activity on the computer's driver port for information about the system. The Python script would react differently based on whether debugging, system identification tests or experiments occurred.

The UART to Serial chip used was the FT230x (USB to BASIC UART IC). It was chosen due to the easy support circuitry it requires with the option to use LED's to indicate any activity on the receive (Rx) & transmit (Tx) communication lines.

The UART to serial circuit was tested by doing a loopback test. The loopback test consist of connecting the Tx and Rx lines together. This results in the circuit echoing anything that the receiver has sent. The schematic of the circuitry is shown in Appendix A.4.

4.2.3 Voltage Regulation

The various components used in the electronic design required different supply voltages and can be seen in Table 4.4.

The 12 V supply was provided using an external bench power-supply and were done converted to 5 V and 3.3 V using linear voltage regulators. The schematic for each voltage regulator is shown in Appendix A.4, and includes a Light Emitting Diode (LED) to ensure the minimum load was met for each regulator. The LED also acts as a visual debugging method.

4.2.4 Potentiometer Sensor

4.2.4.1 Principle of Operation

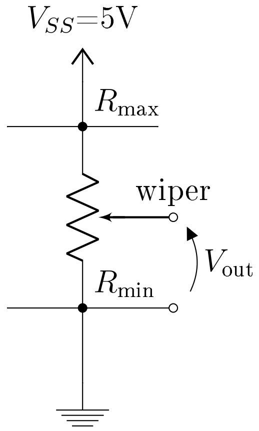

Figure 4.6: Simplified Model of a Potentiometer

The rotary position potentiometer consist out of a wiper that is attached to a rotating shaft. This wiper moves across a internal resistor as the shaft rotates and changes the effective resistance across the output terminal. It provides thus a proportional voltage to its position as seen in Figure 4.6 that indicates the position.

4.2.4.2 Interface

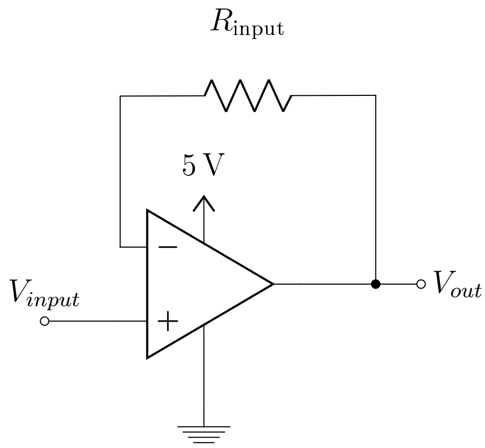

Figure 4.7: Unity Gain Amplifier Circuit

The signal produced by the rotary potentiometer varies from 4.95V and 50mV as it rotates from 360° to 0°. This signal was sent through a simple voltage divider circuit to reduce the signal to 3V and 15mV to be within the sampling limits of the microcontroller. The scaled voltage was then sent through a unity gain rail-to-rail amplifier, where the mirrored output signal is fed into the ADC.

The type of ADC used in the STM32F030C6 is a successive approximation register (SAR) and contains an internal capacitors that suffers from the effect of being depleted if the sampling frequency is too high (stm, 2017). Using an operational amplifier reduces the risk of depleting this internal capacitor because of the low output resistance. The schematic of the circuit is shown in Appendix A.4.

4.2.5 Magnetic Encoder

4.2.5.1 Principle of Operation

A rotating gear containing ferrous metal teeth is attached to the rotating shaft. The rotating metal teeth rotates near a hall-effect sensor which creates a change in the magnetic flux inside the hall-sensor. This change in magnetic flux is sensed by the hallsensor which produces a digital signal (Instruments, 2006).

4.2.5.2 Digital Interface

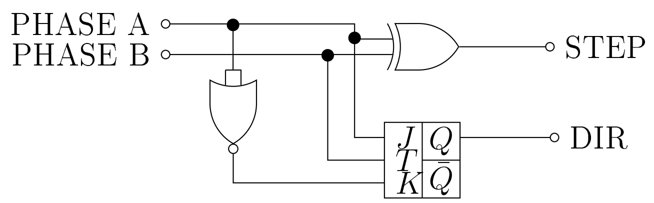

Figure 4.8: Digital Logic Circuit containing JK-Flipflops, XOR- and NOR Gates

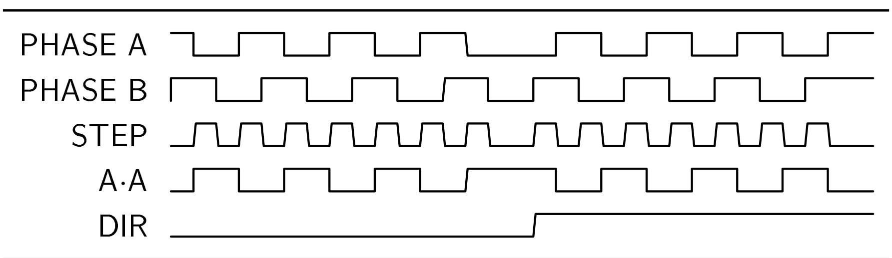

Figure 4.9: Waveform of the JK-Flipflop,XOR, and NOR Gate Circuit

The encoder contains a sold state hallsensor which provides 2 channels with a 90° phase difference between them. (Faulhaber, 2011). These 2 signals under go a hardware decoder that produces 2 signals that indicate the direction of the motor and the incremental position. The hardware filter was implemented to reduce the processing time the microcontroller was required to do to determine the incremental position and the rotational direction.

The hardware filter consists out of a XOR, NOR and JK-Flipflop gates shown in Figure 4.8 and the schematic in Appendix A.4. The XOR gate produces the incremental change of position of the motor which is then read by the microcontroller using interrupts on rising and falling edges. The output of the XOR gate is shown in Figure 4.9.

The resolution of the encoder is 16 lines per revolution per channel, equalling to a combined 64 rising- & falling edges in total. The encoder is connected directly to the motor shaft which speed is reduced by the 14:1 reduction gearbox. The encoder will thus rotate 14 times per output shaft revolution, increasing the resolution to 896 edges per revolution.

The NOR and JK-Flipflop combination produces the direction of the motor by determining whether phase A leads or lags phase B by 90°. This leading or lagging was indicated by a logical 1 or 0 which is read by the microntroller shown in Figure 4.9.

4.2.5.3 Logic Level Converters

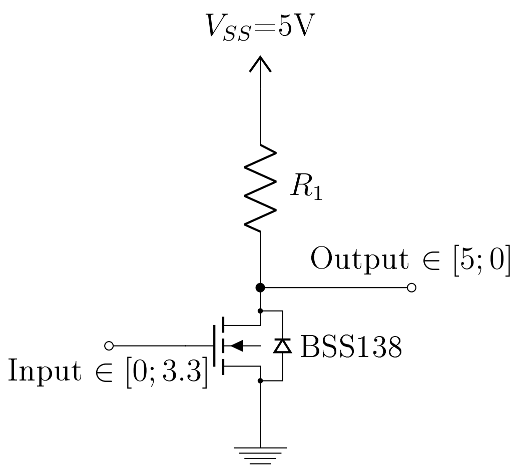

Figure 4.10: Logic Level Converter & Inverter Circuit

The microcontroller is required to interface with the motor driver and represent a logical high and low as a 3.3 V and 0 V respectively. The motor driver's logical high threshold is 3.5 V. It is thus required to use a logic level converter to allow reliable communication between the two devices.

The logic level converter used shown in Figure 4.10 uses the BSS128 transistor. The circuit shown also acts as an inverter where a logic low, 0 V by the micro-controller will be converted to a 5 V and a logic high, 3.3 V will be converted to 0 V. This side effect was overcome by inverting the desired respons es in software.

4.2.5.4 AND Digital Circuit

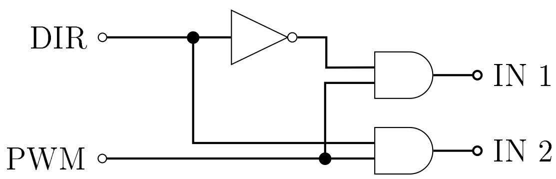

Figure 4.11: AND digital logic with inverter

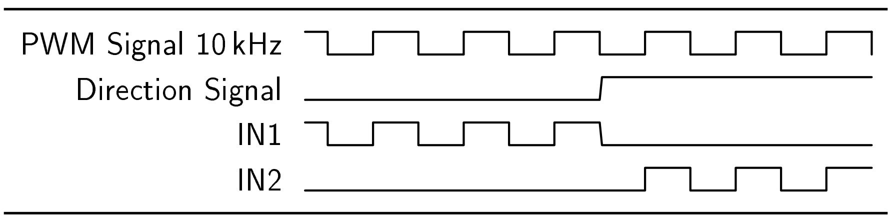

Figure 4.12: AND Digital Logic Circuit Waveforms

The motor driver contains 2 input pins which controls the voltage polarity of the motor terminals. Keeping the one input high and the other low will turn the motor in the one direction and switching the logical values on these inputs will turn the motor on the other direction. Adding speed control requires the PWM signal that the motor receives to be alternated on these inputs and are done by the AND digital circuit.

The AND circuit receives 2 signals from the microcontroller after it has been converted to the correct logic level: the PWM signal and a logic level signal indicating the desired direction. Based on the directional signal the AND circuit will switch the PWM signal between the 2 inputs of the motor driver while holding the other low as seen in Figure 4.12.

to do in order to switch
This hardware directional control was done in order to reduce the processing time the microcontroller was required to do in order to switch the generated PWM signal between the 2 inputs of the motor driver.

4.2.6 Motor Driver

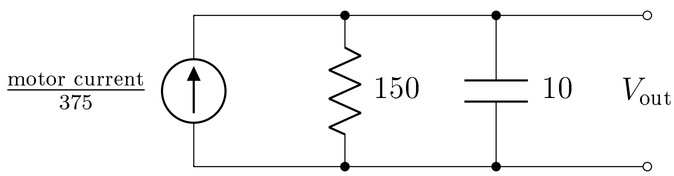

Figure 4.13: Simplified Circuit of Motor Feedback

The motor driver chosen was the MC33887. It was selected based on providing the motor up to 6 A of current, while withstanding the high current transients due to the fast switching of a inductive load (mot, 2007). The motor driver provides the motor with 12V DC which is externally provided by a DC power supply. The schematic of the motor driver is shown in Appendix A.4.

The motor driver is connected directly to the motor and responsible for directional and rotational control of the brushed DC motor. The motor driver contains 2 half H-bridges that forms a full H-bridge which are Pulse-Width-Modulated (PWM) to control the speed of the motor and originates from the microcontroller. The selected frequency was 10kHz and is recommended by the manufacturers (mot, 2007). As discussed previously, the signals' logic level was first converted and then sent through the AND digital filter before the motor driver receives it.

The MC33887 provides a proportional current of $\frac{1}{375}$ of the current flowing through the high-side of the full H-bridge (mot, 2007). This current is sent through a resistor of $150\,\Omega$ to provide a voltage signal to represent the current. Due to the motor being controlled using PWM, the current is a periodic impulse signal making it almost impossible for the ADC to sample. This problem was overcome by adding a parallel capacitor to the resistor to create a ripple voltage. This ripple voltage is sent through an unity-gain amplifier as seen in Figure 4.7 before it is sampled by the micro-controller. The R_{input} resistance is the input resistance that the operational amplifier sees. This closes the feedback loop to implement torque control by the control system.

4.2.7 Verification Tests

4.2.7.1 PWM Duty Cycle to Motor Current

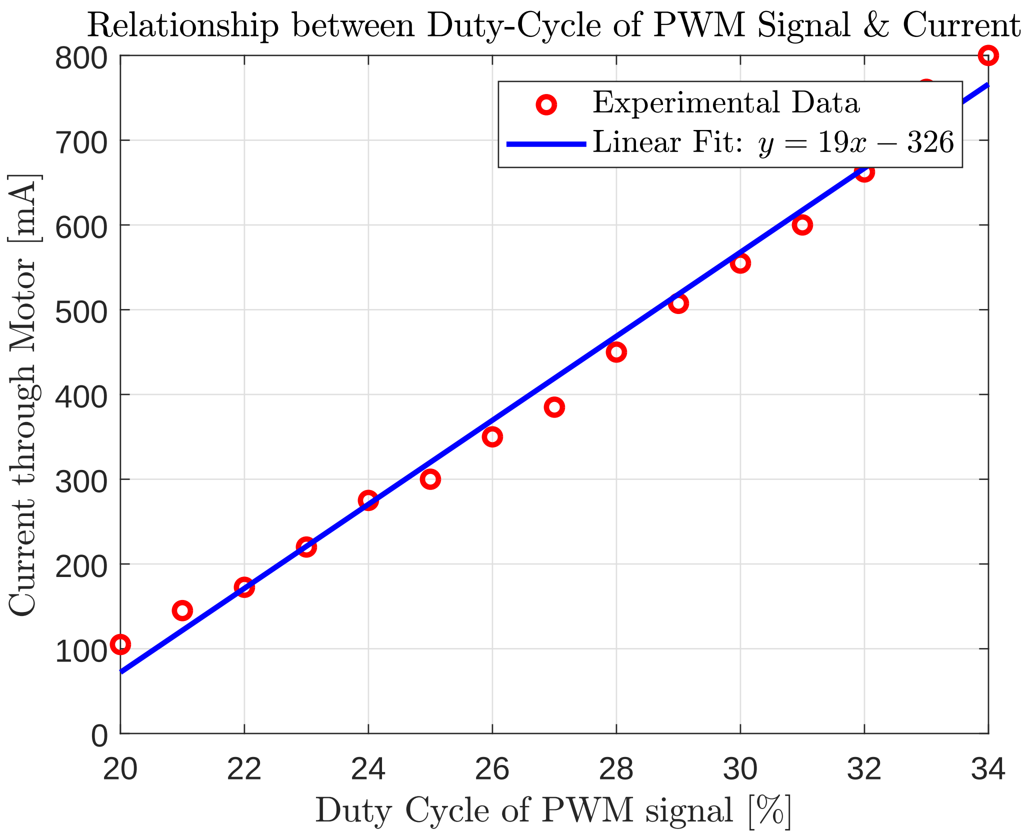

Figure 4.14: Relationship between Duty-Cycle of PWM Signal and Current through Motor

The model describing the system in equation (2.4) assumes the torque delivered to the system is instantaneously available. This is inaccurate is due to the fact that the model describing the DC motor is a second-order differential equation containing its own time constant. This model was not incorporated as adding another control loop would add more delays to the control systems. This was overcome by mapping the torque the motor provided to the duty cycle the motor receives.

Experiments were done to determine the relationship between the duty-cycle of the PWM signal and the torque delivered by the motor. These experiments are done by incrementing the duty-cycle of the PWM signal that the motor receives when the shaft is kept fixed against a hard-stop. The mean value of the output voltage from the circuit shown in Figure 4.13 was measured on the oscilloscope and mapped backwards to determine the torque using

Constant	Description	Value
GR	Gear Ratio	14
FR	Feedback Current Ratio	375
α_t	Torque Constant	19.1×10^{-3}
R	Resistance	150

Table 4.5: Values of Constants used in Equation (4.8)

equation (4.8) with the constants shown in Table 4.5

$$\tau = \frac{V}{R} \cdot GR \cdot FR \cdot \alpha_t \tag{4.8}$$

Figure 4.14 shows the measured data with a line of best fit. It is clear that there exists a linear relationship between the duty-cycle of the PWM signal and the torque provided. This equation of best fit will thus be used to output the correct torque determined by the control system.

Chapter 5

Software Design

[JAPIE]This chapter presents the design and implementation of the software that was executed on the personal computer and on the microcontroller system that controls the robotic gymnast. The software functions include serial communications between the personal computer and the microcontroller, the interfacing with the motor and the angle sensors, the execution of the feedback contol laws, and the logging of the reference commands, the motor commands, and the sensor measurements.

5.1 Software Requirements

The software required to implement the retrieval of system state information, debugging and control laws are presented here. The software design was of crucial importance in the continuation of the project after the simulation phase. The software design allowed the determination of the system characteristic parameters and the verification of the simulation and controller.

5.1.1 Communication

Communication between the external computer and the microcontroller occurred differently based on whether an experiment was done such as system identification or testing different parts of the electronic system. These difference are explained in the following section.

If experiments are conducted the communication are bi-directional between the microcontroller and the external computer. The microcontroller streams the state variables of the system to the external computer in the structure shown in Figure 5.1. The star attached to the variables indicate that they are not sent in the correct units due to sending data types such as floats are computation hungry and are rather handled on the external computer. The external computer will then translate the variables into their correct units and compute the control input based on the control law. The external computer sends the control input back to the microcontroller to output the correct signals.

0	1	2	3	4	5	6	7
$	time	,	θ^*	,	ϕ^*	,	τ^*

Figure 5.1: Data Structure for Streaming Data during Experiments

The structure used in Figure 5.1 was chosen as comma-seperated values (.csv) which makes it easy to write the data in a .csv file to analyse later.

The other state in which communication occurred was used for debugging purposes. In this state the *Python* script allows the user to type commands adhering to the structure shown in Figure 5.2. Based on the command used, the microcontroller would echo the same command back if it completed the command instructed. These commands included to receive the sampled values of signals as well as manual control over the duty-cycle of the PWM signal and directional control of the motor. It also acted as a soft layer for safety by sending commands to arm the system before experiments. A summary of the possible commands are given in Appendix A.5.

`byte`	0	1	2	3	4	...	n-1	n
	$	cmd	,	value	value		\r	\n

Figure 5.2: Data Structure for Sending Commands

5.1.2 Embedded Program

Figure 5.3 shows the main execution flow of the microcontroller based on factors that influence their states. A brief overview of the execution flow is described below.

On startup of the microcontroller, the various peripherals required for operation are initialised. They include timers for PWM generation, ADC for sampling and interrupts for encoder signals. The microcontroller will then initialise the various variables required for operation.

Once initialisation was completed the microcontroller will check via an interrupt if a byte over the serial communication has been received. If a byte has been received, the microncontroller will verify the command structure and execute based on this command.

Every 0.1ms the microcontroller will inspect the data arrays of the sampled signals. Direct Memory Access (DMA) was used for sampling and this results in the sampled data to be automatically refreshed by hardware.

The microcontroller will then react whether an interrupt has occured to indicate a rising or falling edge on the encoder signal. This falling and rising edge indicates an incremental change of the position of the actuated pendulum and the microcontroller will behave accordingly.

The microcontroller will then verify whether it is required to stream the data every 4ms to the external computer for system identification tests.

5.1.3 Controller

The controllers of the swing-up and balancing are implemented on the external computer in a *Python* script and required more information about the system state than what was received from the microcontroller. How this missing information was determined is explained the following section.

The information the swing-up and balancing controllers required was the angular velocity of both the actuated and unactuated pendulum. This information was acquired using numerical differentiation by using the 3-point backwards method shown in equation (5.1).

$$f'(x) \approx \frac{-3f(x) + 4f(x - \Delta t) - f(x - 2\Delta t)}{2\Delta t} \tag{5.1}$$

The swing-up controller implements multiple cosine and sine functions. These functions were discretised into a lookup table up to the accuracy provided by the sensors. The discretisation was done to decrease the processing time done to compute the next control input command.

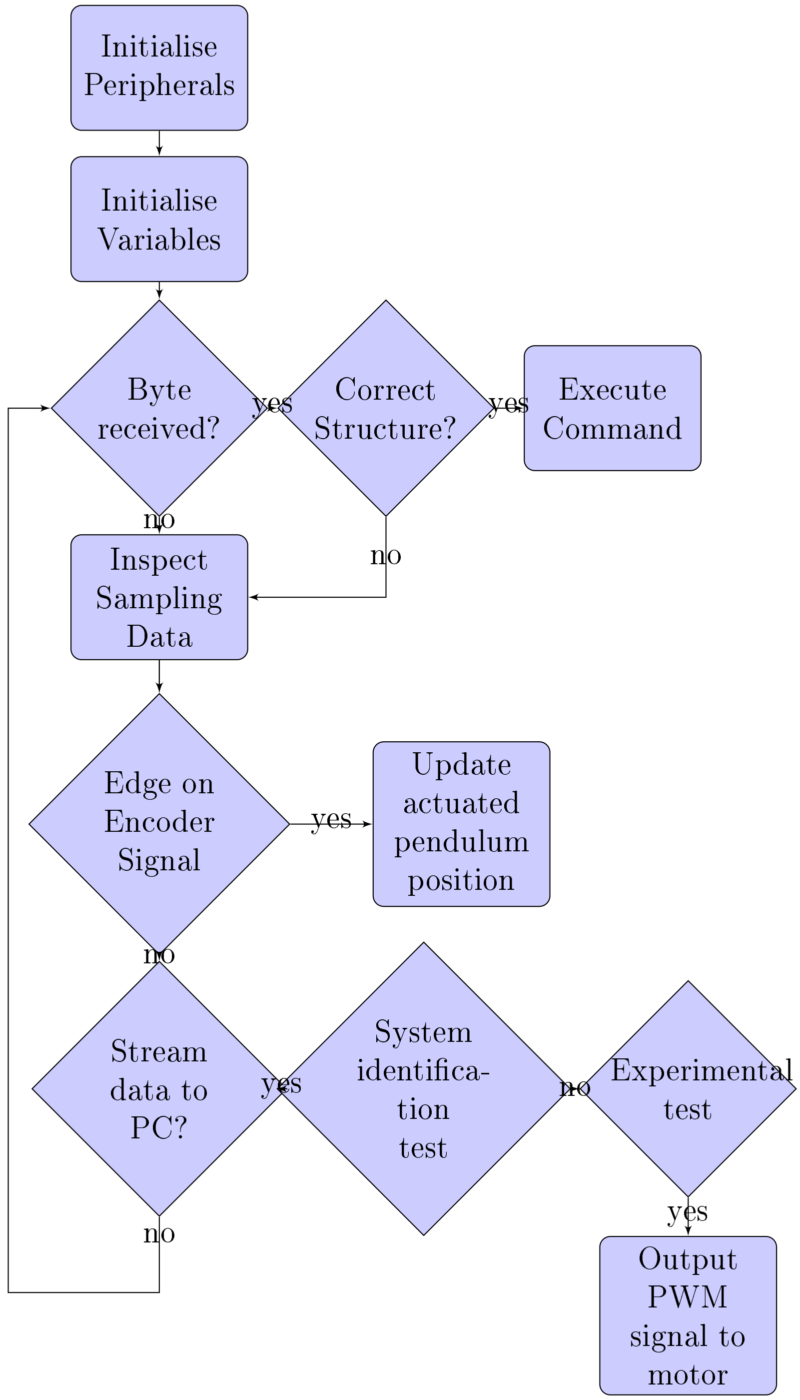

Figure 5.3: Embedded Software Flow

Chapter 6

Conclusion

6.1 Summary

6.2 Recommendation

A short description of the improvements that can be made with regards to *The Feedback Control Of A Robotic Gymnast* is provided in this section, in an attempt to improve the quality of future research.

Choosing a more advanced microcontroller that is able to use a baudrate greater than 115200 would improve response time and provide better control of the system.

Implementing a digital low pass filter to remove the noise on the sampled signal. Especially on the signals that are required to be numerically differentiated.

The script executing on the external computer can be written in a language such as C or C++ to increase the execution time of the script.

6.3 Outcome Assessment

ECSA Exit Level Outcomes	**ELO**	**Section of Report**	**Comment**
Problem Solving	1	2.3 , 2.4, 4.2, 5, 1.4	The project was develop using a system engineering approach. Problems were solved in the simulation program, debugging of issues within the electronic system and implementing the controllers on the external computer
Application of Scientific and Engineering Knowledge	2	2.2, 2.3, 2.4, **??**	The mathematical model was derived and implemented on a simulation program. The system identification was done to identify how to model the system
Engineering Design	3	4.1, 4.2, 5	The mechanical, electronic and sofware designs were done to implement and test the mathematical model
Engineering Methods, Skills and Tools	5	2.3, 4.2, 4.1	MATLAB, Electronic Design Automation (EDA) and Computer-aided Design (CAD) programs were extensively used.
Professional and Technical Communication	6	1 - 6	The writing of the report to present the results of the project, an oral exam towards a engineering audience and creating a poster for a community
Individual, Team and Multidisciplinary Working	8	1-6	The main objectives were achieved on time with supervision throughout the year from a study leader
Independent Learning Ability	9	1.3, 3	Research on the various approaches were done and then implemented

Appendices

Appendix A

A.1 Derivation of the Mathematical Model

From the free body diagram shown in Figure 2.1 the position of the center of mass of the unactuaded and actuaded pendulum can be determine as seen in equation (A.1), (A.2) , (A.3) and (A.4) respectively.

$$x_1 = l_1 \cos(\theta) \tag{A.1}$$

$$y_1 = -l_1 \sin(\theta) \tag{A.2}$$

$$x_2 = L_1 \sin(\theta) + l_2 \sin(\theta + \phi) \tag{A.3}$$

$$y_2 = -L_1 \cos(\theta) - l_2 \cos(\theta + \phi) \tag{A.4}$$

The Lagrange is defined as

$$\mathcal{L} = T - V$$

where T is the potential energy in the system and V the kinetic energy.

The kinetic energy in the system consist of the fixed rotation of the unactuated pendulum and the rotation and velocity of the actuated pendulum.

$$T = \frac{1}{2} I_A \dot{\theta}^2 + \frac{1}{2} I_B (\dot{\theta} + \dot{\phi})^2 + \frac{1}{2} m_2 V_2^2 \tag{A.5}$$

The potential energy in the system is defined as

$$V = -m_1 g l_1 \cos(\theta) - m_2 g [L_1 \cos(\theta) + l_2 \cos(\theta + \phi)]$$

The velocity term V_2 in equation (A.5) must be expanded and this is accomplished by taken the derivative of equations (A.3) and (A.4).

$$\dot{x_2} = L_1 \cos(\theta)\dot{\theta} - l_2 \cos(\theta + \phi)(\dot{\theta} + \dot{\phi})$$

$$\dot{y_2} = L_1 \sin(\theta)\dot{\theta} + l_2 \sin(\theta + \phi)(\dot{\theta} + \dot{\phi})$$

The V_2 term is the magnitude of the velocity of the actuated pendulum and results in the following expansion:

$$x_2^2 = L_1^2 \cos(\theta)^2\theta^2 + l_2^2 \cos(\theta + \phi)^2(\dot{\theta} + \dot{\phi})^2 + 2L_1 l_2\dot{\theta}(\dot{\theta} + \dot{\theta}) \cos(\theta) \cos(\theta + \phi)$$

$$y_2^2 = L_1^2 \sin(\theta)^2\theta^2 + l_2^2 \sin(\theta + \phi)^2(\dot{\theta} + \dot{\phi})^2 + 2L_1 l_2\dot{\theta}(\dot{\theta} + \dot{\theta}) \sin(\theta) \sin(\theta + \phi)$$

$$\begin{aligned} V_2^2 = x_2^2 + y_2^2 = \\ & L_1^2\theta^2[\cos(\theta)^2 + \sin(\theta)^2] + l_2^2(\dot{\theta} + \dot{\phi})^2[\cos(\theta + \phi)^2 + \sin(\theta + \phi)^2] + \\ & 2L_1 l_2\dot{\theta}(\dot{\theta} + \dot{\phi})[\cos(\theta) \cos(\theta + \phi) + \sin(\theta) \sin(\theta + \phi)] \end{aligned} \tag{A.6}$$

Using the following trigonometric identities

$$\cos(\gamma)^2 + \sin(\gamma)^2 = 1$$

$$\cos(\gamma) \cos(\alpha) + \sin(\gamma) \sin(\alpha) = \cos(\gamma - \alpha)$$

the equation (A.6) resolves to:

$$V_2^2 = L_1\dot{\theta}^2 + l_2^2(\dot{\theta} + \dot{\phi})^2 + 2L_1 l_2(\dot{\theta} + \dot{\phi})\dot{\theta} \cos(\phi)$$

The kinectic energy in the system is then defined as:

$$T = \frac{1}{2}I_A\dot{\theta}^2 + \frac{1}{2}I_B(\dot{\theta} + \dot{\phi})^2 + \frac{1}{2}m_2[L_1\dot{\theta}^2 + l_2^2(\dot{\theta} + \dot{\phi})^2 + 2L_1 l_2(\dot{\theta} + \dot{\phi})\dot{\theta} \cos(\phi)]^2$$

and results in the Lagrangian to be:

$$\mathcal{L} = \frac{1}{2}I_A\dot{\theta}^2 + \frac{1}{2}I_B(\dot{\theta}+\dot{\phi})^2 + \frac{1}{2}m_2[L_1\dot{\theta}^2 + l_2^2(\dot{\theta}+\dot{\phi})^2 + 2L_1 l_2(\dot{\theta}+\dot{\phi})\dot{\theta} \cos(\phi)]^2 + m_1 g l_1 \cos(\theta) +$$

$$m_2 g[L_1 \cos(\theta) + l_2 \cos(\theta + \phi)]$$

The differential equation describing the dynamics of the system is

$$\frac{d}{dt}\frac{\partial \mathcal{L}}{\partial \vec{\dot{q}}} - \frac{\partial \mathcal{L}}{\partial q} = B(\dot{q}) + \tau(q)$$

where $q = \begin{bmatrix} \theta \\ \phi \end{bmatrix}$

The appropriate derivatives are done and results in the equations

$$\frac{\partial \mathcal{L}}{\partial \theta} = -m_1 g l_1 \sin(\theta) - m_2 g L_2 \sin(\theta) - m_2 g l_2 \sin(\theta + \phi) \tag{A.7}$$

$$\frac{d}{dt}\frac{\partial \mathcal{L}}{\partial \dot{\theta}} = \\ I_A\ddot{\theta} + I_B\ddot{\theta} + I_B\ddot{\phi} + m_2L_1^2\ddot{\theta} + m_2l_2^2\ddot{\theta} + \\ m_2l_2\ddot{\phi} + 2m_2L_1l2\ddot{\theta}\cos(\phi) - \\ 2m_2L_1l_2\dot{\theta}\dot{\phi}\sin(\phi) + \\ m_2L_1l_2\ddot{\phi}\cos(\phi) - m_2L_1l_2\dot{\phi}^2\sin(\phi) \tag{A.8}$$

$$\frac{\partial \mathcal{L}}{\partial \phi} = -m_2L_1l_2(\dot{\theta}+\dot{\phi})\dot{\theta}\sin(\phi) - m_2gl_2\sin(\theta+\phi) \tag{A.9}$$

$$\frac{d}{dt}\frac{\partial \mathcal{L}}{\partial \dot{\phi}} = \\ I_B\ddot{\theta} + I_B\ddot{\phi} + m_2l_2^2\ddot{\theta} + m_2l_2^2\ddot{\phi} + m_2L_1l_2\ddot{\theta}\cos(\phi) - m_2L_1l_2\dot{\theta}\dot{\phi}\sin(\phi) \tag{A.10}$$

$$\frac{\partial \mathcal{L}}{\partial \phi} = -m_2L_1l_2(\dot{\theta}+\dot{\phi})\dot{\theta}\sin(\phi) - m_2gl_2\sin(\theta+\phi) \tag{A.11}$$

$$\frac{d}{dt}\frac{\partial \mathcal{L}}{\partial \dot{\phi}} = I_B\ddot{\theta} + I_B\ddot{\phi} + m_2l_2^2\ddot{\theta} + m_2l_2^2\ddot{\phi} + m_2L_1l_2\ddot{\theta}\cos(\phi) - m_2L_1l_2\dot{\theta}\dot{\phi}\sin(\phi) \tag{A.12}$$

A.2 Taylor Series Expansion Around Unstable Equilibrium Position

The linearisation of equations (2.3) and (2.4) is by applying the Taylor Series Expansion at the working point:

$$F(\vec{q},\dot{\vec{q}},\ddot{\vec{q}}) \approx F(\vec{q_s},\dot{\vec{q_s}},\ddot{\vec{q_s}}) + \Delta(\vec{q},\dot{\vec{q}},\ddot{\vec{q}}) \cdot \nabla F(\vec{q_s},\dot{\vec{q_s}},\ddot{\vec{q_s}}) \tag{A.13}$$

where the working point is defined as

$$[\vec{q_s},\dot{\vec{q_s}},\ddot{\vec{q_s}}]^T = [\pi,0,0,0,0,0] \tag{A.14}$$

and

$$\Delta(\vec{q},\dot{\vec{q}},\ddot{\vec{q}}) = [\vec{q},\dot{\vec{q}},\ddot{\vec{q}}] - [\vec{q_s},\dot{\vec{q_s}},\ddot{\vec{q_s}}] \tag{A.15}$$

This results in the linearisation of equations (2.3) and (2.4) as :

$$(I_A + I_B + m_2L_1^2 + m_2l_2 + 2m_2L_1l_2)\Delta\ddot{\theta} + (I_B + m_2l_2^2 + m_2L_1l_2)\Delta\ddot{\phi} \\ + (-m_1gl_1 - m_2gL_1 - m_2gl_2)\Delta\theta - m_2gl_2\Delta\phi + f_{c1}\Delta\dot{\theta} = 0 \tag{A.16}$$

$$(I_B + m_2l_2^2 + m_2L_1l_2)\Delta\ddot{\theta} + (I_B + m_2l_2^2)\Delta\ddot{\phi} \\ - m_2gl_2\Delta\theta - m_2gl_2\Delta\phi + f_{c2}(\Delta\dot{\phi} - \Delta\dot{\theta}) = \tau \tag{A.17}$$

A.3 Additional Simulation Results

A.4 Electronic Design Schematic

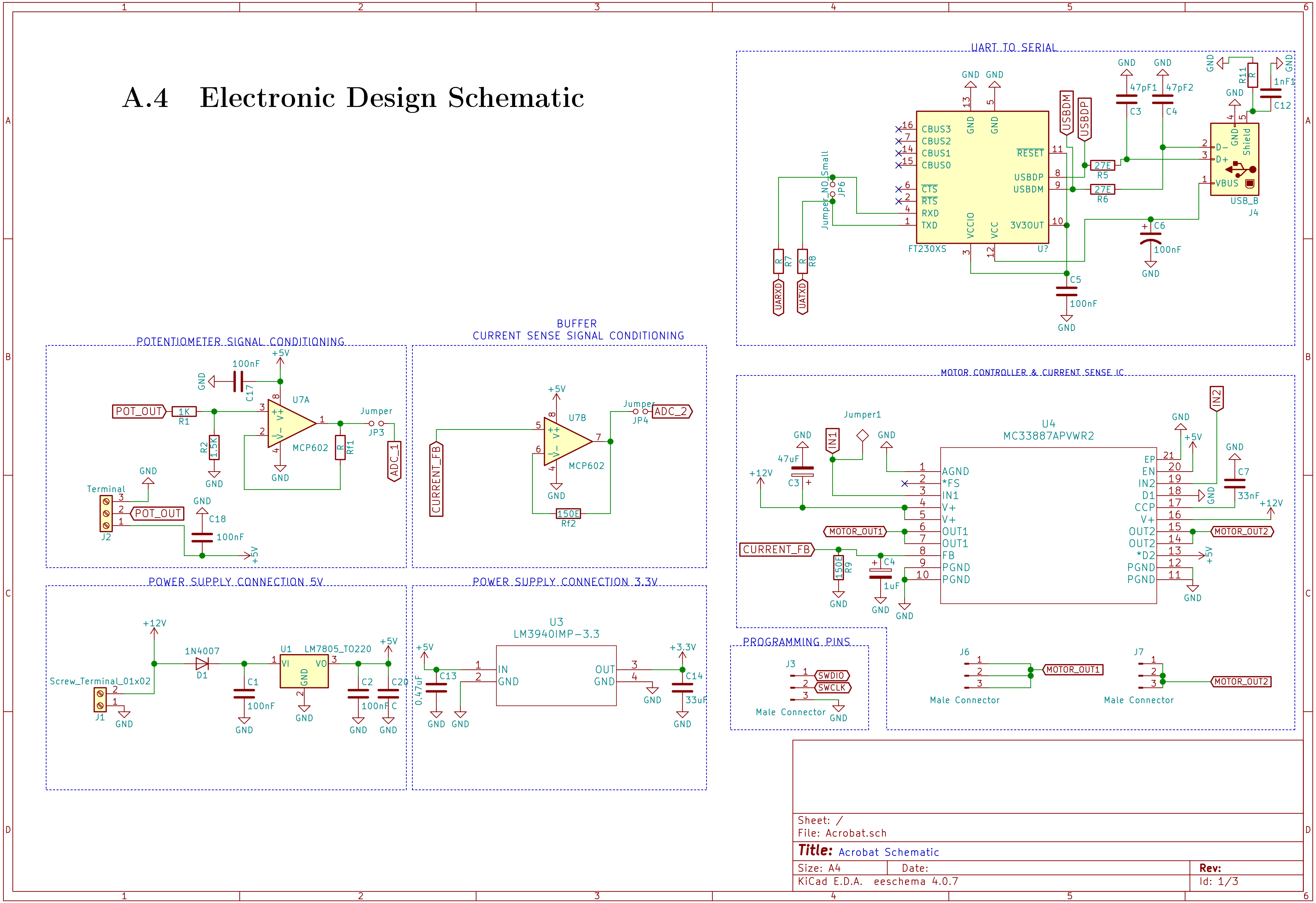

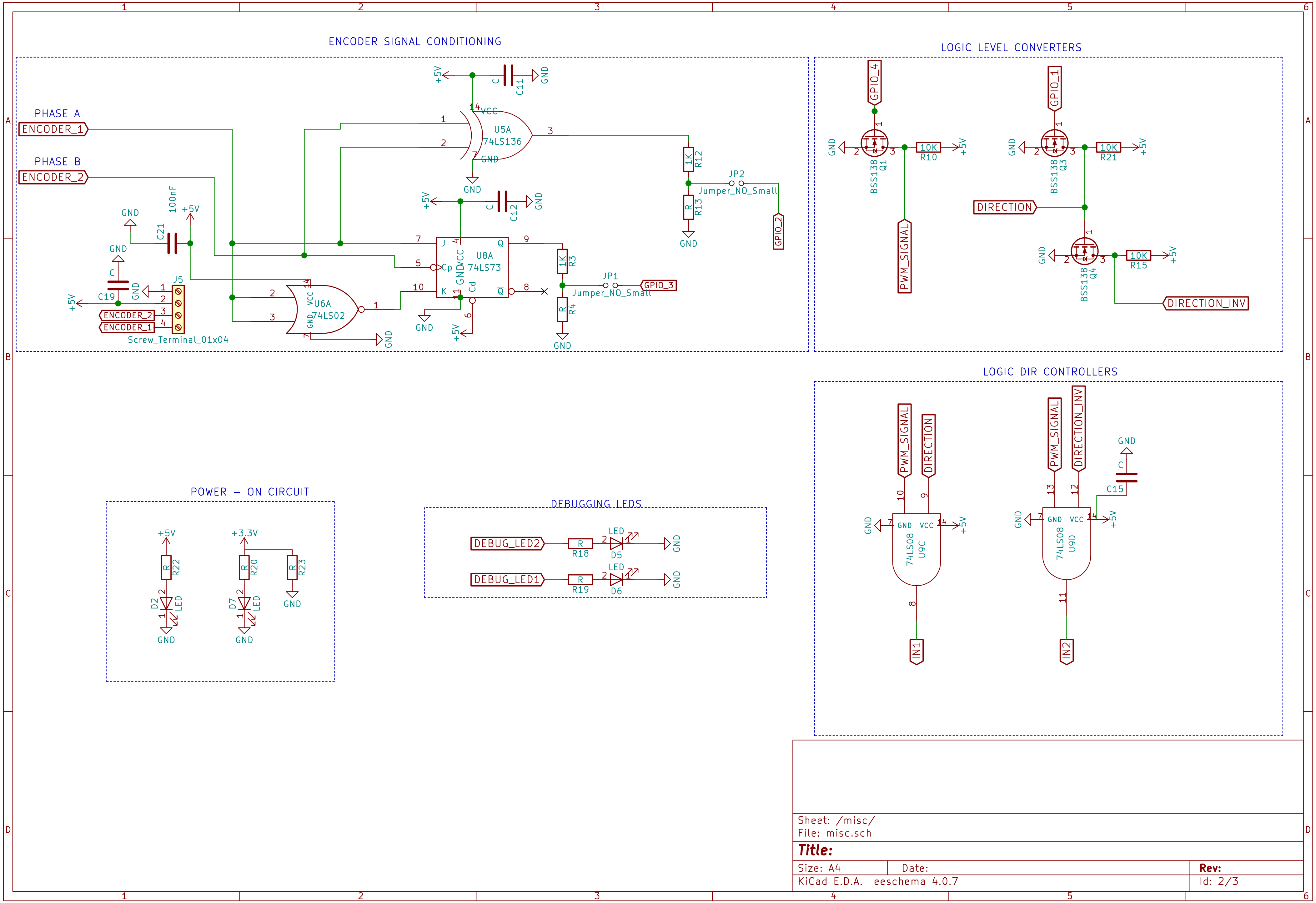

Sheet: /misc/
File: misc.sch

Title:

Size: A4	Date:	**Rev:**
KiCad E.D.A. eeschema 4.0.7		Id: 2/3

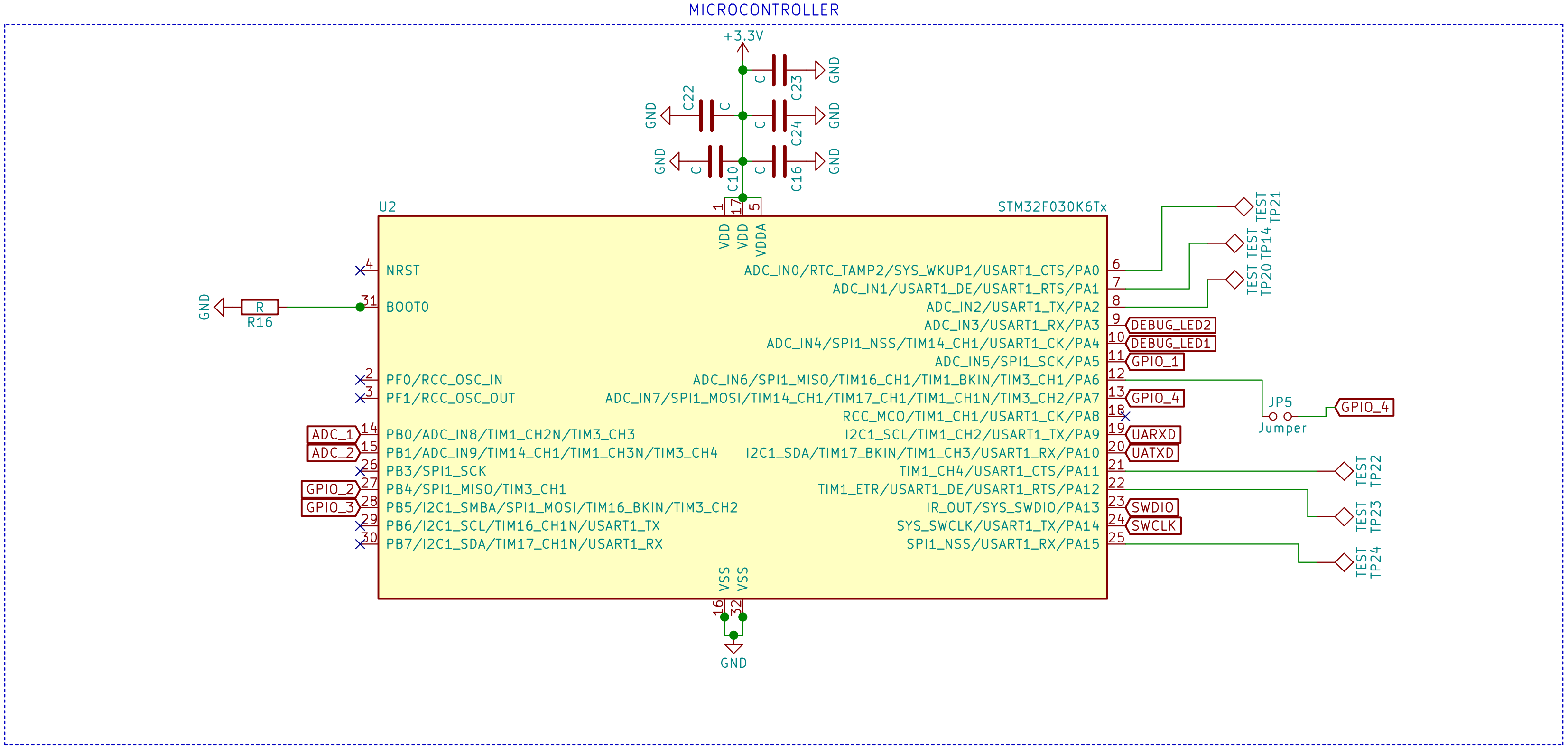

Sheet: /microcontroller/
File: microcontroller.sch

Title:

Size: A4 | Date: | **Rev:**

KiCad E.D.A. eeschema 4.0.7 | Id: 3/3

A.5 Communication Structure

`byte`	0	1	2	3	4	...	n-1	n
	$	cmd	,	value	value		\r	\n

Figure A.1: Data Structure for Sending Commands

In Table A.1 the various commmands that are used in the command structure shown in Figure A.1 used for debugging purposes is explained with the possible value ranges that can be used.

Command	Range	Reason for Implementation	Effect
A	None	Testing of the UART circuit	Send the following text: Feedback Control Of Robotic Gymnast
B	0-1	Used during experiments and system identification tests	Enable streaming of state variables across UART
F	0-100	Testing AND digital circuit and speed control of motor	Changes PWM Duty-Cycle
I	0-1	Testing of AND digital circuit and directional control of motor	Change the rotational direction
X	None	Soft layer for safety	Stops all operation of microcontroller. A powercycle is required.

Table A.1: Summary of Communication Commands and their Effects

A.6 Techno-Economy Assessment

A.6.1 Budget

The comparison between the proposed and actual budget is discussed and why the project was under-budget.

The proposed budget for the project was R3000. This budget was required to cover manufacturing cost and the buying of sensors, equipment and components. Table A.2 provides the categories and amount of what the project consisted out of.

Category	Cost
Electronic Components	R100
Mechanical Components	R300
Software	R0
Mechanical Manufacturing	R0
Electronical Manufacturing	R0
Total	R200

Table A.2: Categories of the Budget

It is visible from the budget that the project is under-budget. The reason for being under-budget is due the Electrical and Electronic (E&E) Deparment providing the service and components which were most expensive. This includes the manufacturing cost of the mechanical and electronic design and the Mechanical and Mechatronic Department providing the most expensive mechanical component.

A.6.2 Planning

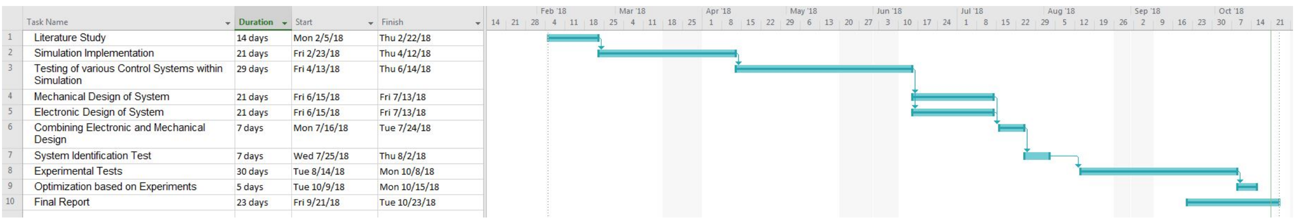

Figure A.2: Planned Gantt Chart of the Project

Figure A.2 shows the Gantt chart for the planned activities during the project. For the majority of the project, the planned activities were followed

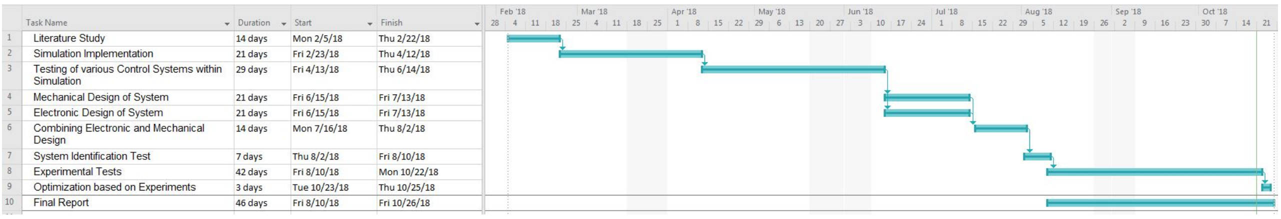

Figure A.3: Actual Gantt Chart of the Project

Task Name	Planned Hours	Actual Hours
Literature Study	10	11
Simulation Implementation	15	12
Testing & Verification of Simulation	20	20
Mechanical Design	50	51
Electronic Design	50	57
System Identification Test	2	2
Experiments	2	
Writing of Report	84	2

Table A.3: Hours worked during the different phases of the project

as planned. These activities include the literature study up to the combining of the electronic and mechanical designs.

During the experimental testing it was required to improve the mounting method between the motor shaft and the actuated pendulum. During this modification the experiments could not continue and additional time was required to complete it. The decision to extend the time required for the experiments were justified by the increase of safety to the individual and surroundings during experiments. It was also decided that during the improvement of the mounting method the writing of the report started.

The electronic design took longer than what was planned due to experiencing difficulty programming the theoretical controllers on the microcontroller. It was decided to extend the time required for this phase due to without the controllers no practical results of these controllers would be acquired. It was decided to take an additional week to implement the controllers.

A.6.3 Technical Impact

The impact of the results presented in this report on the field of control systems, society and industry are discussed and whether the financial input was worthwhile.

The problem of the swinging and balancing of the robotic gymnast is a well researched problem. Solutions to the swinging and balancing are provided on a theoretical level and supported by simulation results however little practical results are available of these theoretical solutions. The impact of this report on the field of control systems includes the practical results of one of these theoretical solutions and discusses how the practical results differ from the theoretical results.

The impact of the practical results of this report on the industry of underactuated robotics are little. The robotic gymnast is a interesting problem and consist out of a highly non-linear and linear behaviour and is rather consider a great introductory problem to the field of underactuated robotics. Method used for controlling underactuated robotics are more advance and build on the techniques describe in this report.

The impact of this report has little impact on society due to being of little interest to the industry. The industry will not use the results and discussion presented in this report due to the reasons mentioned in the previous paragraph.

The financial input was worthwhile due to providing practical results on one theoretical implementation to the swinging and balancing of the robotic gymnast. There exist rather little practical results of the controller presented in the report and the report provides a discussion between the simulated behaviour and practical behaviour.

A.6.4 Return on Investment

The short and long term value from a technical and economical perspective is provided in this section. A motivation on the continuing research in the field of underactuated robotics are given and the financial cost to further research in this field.

Researching underactuated robotics is a exciting and growing research field due to the field of underactuated robotics have increasingly become more important due to technology growing in areas where control is crucial. Areas include: air drones, underwater inspection vehicles, space exploration and the aeroplane industry.

Underactuated robotics is an interesting and open field in control, with many design options to approach these types of problems. The most interesting examples of underactuated control problems are legged, swimming and flying robots that has been mentioned in the previous paragraph. This results in underactuated robotics being relevant in many fields.

The economical value of underactuated robotics in the short term and long term is high. Products are being brought to market that solve very difficult problems and can be used in a broad variety. These products include *Spot* from *Boston Dynamics* which can be used for inspection, transportation and entertainment. The market is open for more competitors to enter and results in having long term value.

The financial cost to further the research on underactuated robotics are low due to the use of simulation programs that allows the testing of solutions on realistic simulated models. This significantly reduce the number of prototypes required to test the solution practically.

A.6.5 Potential for Commercialisation

The potential for the commercialisation of the contents within the report is discussed and the value of this commercialisations is given.

The contents does not have any real value for commercialisation. As mentioned earlier the problem researched is a very good introductory to underactuated robotics due to containing techniques that is a foundation for more advanced problems.

A.7 Risk Analysis & Safety Procedures

BEng(Mechatronic) Safety Report

Experimental Test of the Swinging and Balancing of the Robotic Gymnast

Date: August 2018

Supervisor: Dr. J.A.A Engelbrecht

Student: Henry Kotzé

Laboratory Technician: Henry Kotzé

Emergency Contacts:

Contact	Room nr.	Work nr.	Cell nr.
Mr. Ferdi Zietsman	M212	021 808 4954	083 233 1646
Dr. J.A.A Engelbrecht	E417	021 808 4334	-
Campus Security	-	021 808 2233	-
Fire Brigade	-	021 887 1333	-
Ambulance	-	021 883 3444	-

Pressure Vessels or Pipes: No pressure vessel or pipe with a pressure in excess of 50 kPa is involved in - this project

----

Laboratory Technician (Henry Kotzé)

Supervisor (Dr. J.A.A Engelbrecht)

Laboratory Manager (Mr Cobus Zietsman)

<u>Overview of Testing:</u>

The feedback control system responsible for the swinging and balancing of the robotic gymnast is to be tested. The purpose of the tests is to determine if the controllers can swing the robotic gymnast from the stable equilibrium position (hanging downwards) to the unstable equilibrium position (balancing inverted).

The tests are required to test whether the model on a simulation program is a true representation of the physical model.

The equipment to be used is detailed as follows:

Equipment:
Bench Power Supply (max current of 3 A)
External Computer
G Clamps
Oscilloscope

<u>General Lab Safety</u>

The following general lab safety instructions are applicable:

- No afterhours testing may be performed without the necessary permissions.
- An induction is required before testing may be undertaken.
- Closed shoes must always be worn.
- Loose clothing may not be worn.
- Good housekeeping practices should be kept during testing.
- No food or drink is permitted in the lab.
- Extreme caution should be taken when working in the DIC lab as this lab houses sensitive optical equipment that may not be bumped, dropped or otherwise violently disturbed.
- Safety report must be visible and accessible during testing

<u>Activity Based Risk Assessment</u>

Activity	**Risk**	**Risk Type**	**Mitigating Steps**
Entering the laboratory	Injuring hand from door	P	Ensure hands are removed from the closing path of the door
Powering on the equipment	Electrical Shock	P	Inspect the condition of cable insulation and whether it is connected properly and to correct port.

Moving around in the laboratory	Falling over objects	P	Investigate the environment and be aware of objects on the ground
Mounting base with G-clamp	Crushing fingers	P	Ensure hands are out of the gripping direction of clamp
	Dropping the g-clamp	E	Be cautions when working with G-clamp
Swinging of Robotic Gymnast	Being strike by pendulums	P	Be outside the plane of rotation during tests. Enclosed test area with warning tape
	Pendulum striking G-clamp	E	Ensure G-Clamp is outside of the plane of rotation of pendulum
Inspecting hard stops	Being strike by Pendulums	P	Switch off all equipment and remove cables from ports
Inspecting Coupling	Being strike by Pendulums	P	Switch off all equipment and remove cables from ports
Balancing of Robotic Gymnast	Being strike by Pendulums	P	Be outside the plane of rotation during tests. Enclosed test area with warning tape
	Pendulum striking G-clamp	E	Ensure G-Clamp is outside of the plane of rotation of pendulum
Data acquisition	Data loss	P	Ensure the correct file format is selected
Tightening grub screw of shaft	Stripping the thread	E	Be cautious when tightening the screw to the shaft.
Inspecting the grub screw	Being strike by Pendulums	P	Switch off all equipment and remove cables from ports
Powering down equipment	Electrical Shock	P	Inspect the condition of cable insulation and whether it is connected properly.
Exiting the laboratory	Injuring hand from door	P	Ensure hands are removed from the closing path of the door

List of References

(2007 2). 5.0 A H-Bridge woth Load Current Feeback. Freescale Semiconductor, 12th edn. Document Number: MC33887.

(2017). How to get the best ADC accuracy in the STM32 microcontrollers. ST Electronics.

Brown, S.C. and Passino, K.M. (1997). Intelligent Control for an Acrobot. Journal of Intelligent and Robotic Systems, vol. 18, no. 3, pp. 209–248. ISSN 09210296.
Available at: `http://link.springer.com/10.1023/A:1007953809856`

Faulhaber (2011). Encoders, Magnetic Encoder, Series IE2-16. Faulhaber, 11th edn.

Gene F. Franklin, J. David Powell, e.a. (2015). Feedback Control of Dynamic Systems. 7th edn. Pearson Education Limited, Edingburgh Gate, Harlow, Essex CM20 2JE, England. ISBN 1-29-206890-6.

Inman, D.J. (2015). Engineering Vibration. Pearson Education Limited.

Instruments, N. (2006 9). Magnetic Encoder Fundamentals. 10. National Instruments, The address.

Lehl, M. (2012 10). Control Of Planar Pendulum Systems. Ph.D. thesis, Technische Universität München.

Murray, R.M. and Hauser, J. (1991). A Case Study in Approximate Linearization: The Acrobot Example. Tech. Rep..
Available at: `http://www.cds.caltech.edu/ murray/preprints/erl-M91-46.pdf`

Spong, M.W. (1995). The Swing Up Control Problem For The Acrobot. IEEE Control Systems. ISSN 1066033X.

Tedrake, R. (2009). Underactuated robotics: Algorithms for walking, running, swimming, flying, and manipulation (course notes for mit 6.832).
Available at: `http://underactuated.mit.edu/`